Composites Part B 174 (2019) 106947

Contents lists available at ScienceDirect

Composites Part B

journal homepage: www.elsevier.com/locate/compositesb

Organic versus inorganic matrix composites for bond-critical strengthening applications of RC structures – State-of-the-art review

Hussein M. Elsanadedy *, Husain Abbas, Tarek H. Almusallam, Yousef A. Al-Salloum

Chair of Research and Studies in Strengthening and Rehabilitation of Structures, Dept. of Civil Eng., College of Eng, King Saud University, P.O. Box 800, Riyadh, 11421, Saudi Arabia

ARTICLE INFO

Keywords:
Organic matrix composites
Fiber reinforced polymers
Inorganic matrix composites
Fabric reinforced cementitious matrix
Textile reinforced mortar
Flexural strengthening
Shear strengthening
Concrete structures

ABSTRACT

The usage of organic matrix composites such as fiber reinforced polymers (FRP) in retrofitting of structures is increasingly becoming popular among structural designers, which is credited to varied attractive top features of these materials, such as: corrosion resistance, higher strength to weight ratio, ease and speed of application, and almost no section enlargement. However, FRP strengthening technique is not completely free of problems. The organic resins employed as binders have many disadvantages such as (a) relatively expensive resins; (b) poor response at temperature ranges above the glass transition temperature; (c) potential risks for the workers; (d) difficulty in application on moist areas or at low temperature ranges; (e) difficulty of reversibility (inability to undo the repair without damaging the original structural member); and (f) non-compatibility between resins and substrates. One possible solution for alleviating these difficulties is the substitution of the organic with the inorganic binder, such as cementitious mortars. A new class of material was then developed and used for structural strengthening applications. In this material, fibers are replaced by textile or fabric and organic matrix is replaced by cementitious matrix such as mortars and is usually called textile reinforced mortar (TRM). This paper presents a critical review of existing research on comparison between FRP and TRM composites used for strengthening of structural concrete members, identifies gaps in current knowledge, and outlines directions for future research. It briefly presents material characterization in terms of constituents and stress-strain behavior in tension, and also describes concisely methods of installation for both organic and inorganic composite systems. Available literature on bond behavior at composites-to-concrete interface at ambient and elevated temperatures are summarized. It also enlists available research on use of TRM composites in comparison with FRP composites for flexural and shear strengthening of RC beams.

1. Introduction

The strengthening of existing concrete structures is frequently required due to any one or combination of the following reasons: (i) increase in load because of the increase in live loads, increase in wheel loads, or planning to install heavy machines; (ii) damage caused to the structure because of aging of building materials, fire exposure, corrosion of steel rebars, and/or vehicle crash against structure; (iii) changes in the structural system because of the removal of load bearing walls/columns and/or cutting openings through slabs for services; (iv) mistakes in structural planning or construction leading to inadequate member sizes and/or inadequate rebars; or (v) seismic retrofit to comply with current seismic design codes.

Most common strengthening methods for concrete structural members include: section modification, external post-tensioning of members, bonding of steel plates, steel jacketing, insertion of near surface mounted (NSM) steel or glass fiber reinforced (GFRP) bars, and the use of externally bonded fiber reinforced polymer (FRP) laminates [1–18]. These techniques are briefly discussed below.

Section enlargement is the easiest and simplest upgrading scheme (Fig. 1(a) [19]). An essential component for this scheme is the monolithic action of the section [20]. However, the efficient addition of capacity requires sufficient increase in the sections, which reduces clearances and adds additional weight. Moreover, the placing of formwork and the fabrication of rebar cage is labor intensive [3].

External post-tensioning requires the use of prestressing tendons or bars to carry the additional loads (Fig. 1(b) [21]). Post-tensioning is one of the most effective options for retrofitting as it has minimum

* Corresponding author. On leave from Helwan University, Cairo, Egypt.
E-mail address: elsanadedy@yahoo.com (H.M. Elsanadedy).

https://doi.org/10.1016/j.compositesb.2019.106947
Received 28 January 2019; Received in revised form 8 May 2019; Accepted 27 May 2019
Available online 29 May 2019
1359-8368/

intrusiveness and does not cause significant reduction in clearance. Nevertheless, the disadvantages of this technique include susceptibility to corrosion of steel bars/tendons, poor fire performance of FRP tendons, high cost of tendons, and vulnerability to vandalism [4].

Another popular approach to strengthening requires the use of externally attached steel plates, which can be bonded or anchored to the members allowing the transfer of forces (see Fig. 1(c) [22]). Advantages that are associated with this technique are: no requirement of skilled labor, ductile behavior, less disruption, and cost effectiveness [23]. However, the disadvantages of this technique include susceptibility of steel plates to corrosion, reduced clearances, increased weight due to heavy retrofitting materials.

Another approach to strengthening RC structural members is the employment of near surface mounted (NSM) bars, which requires the laying of steel or FRP bars in the grooves cut in the concrete cover and filling the grooves with a cementitious or epoxy-based mortar (see Fig. 1(d) [24]). Due to the availability of high quality epoxies and FRP composites, the steel bars are getting replaced by FRP in the design of NSM system for the retrofitting of structures [25].

For the last more than three decades, fiber-reinforced polymer (FRP) composites are steadily gaining recognition as suitable replacement of steel in the retrofitting of concrete structures (Fig. 1(e) [26]). This is because of the beneficial properties of the FRP composites such as corrosion resistance, sufficiently high strength-to-weight ratio, speed and ease of application, minimum alteration in the geometry, and minimum disruption of services [27]. Despite these advantages, the FRP retrofitting methods have some drawbacks as well, that are related to the resins employed in binding of fibers [28–30]. These disadvantages include: a) de-bonding between FRP and concrete substrate; (b) poor response of epoxy resins at elevated temperature when it is more than the glass transition temperature; (c) expensive epoxies; (d) difficulty in applying FRP on damp concrete areas or at low temperature ranges; (e) insufficient vapor permeability, that may damage the concrete members; (f) lack of compatibility between substrate materials and epoxy resins; (g) difficulty in carrying out post-earthquake evaluation of the damage caused to concrete behind intact FRP laminates.

Fig. 1. Examples of strengthening techniques of concrete structures: (a) Section enlargement [19]; (b) External post-tensioning [21]; (c) Steel plate bonding [22]; (d) NSM strengthening [24]; (e) FRP strengthening [26]; (f) TRM strengthening [31].

One possible remedy for the above mentioned difficulties in using FRP laminates for strengthening may be the use of inorganic binders (e.g. cementitious mortars) in place of organic binder thereby resulting in the substitution of FRP with fiber reinforced mortars (FRM). Because of the granularity of the mortar, penetration of fibers is hard to attain. Moreover, the cementitious mortars cannot moist all fibers. Enhanced fiber-matrix bonding may be attained by using fiber textile instead of fiber sheets. The textiles consist of fabric meshes produced from fiber rovings, which may be knitted, woven, or unwoven. Consequently, new materials have been recently emerged for circumventing the issues associated with FRPs [31]. These materials are known by different names such as inorganic matrix composites, textile reinforced mortar (TRM), fabric reinforced cementitious matrix (FRCM) systems, textile reinforced concrete (TRC), or mineral-based composite (MBC) systems. Examples of retrofitting of concrete structures using textile reinforced mortar are given in Fig. 1(f) [31].

While various review articles were found in literature on existing research on the performance of FRP-strengthened RC structural elements under ambient and elevated temperature environments [e.g. [32–36]], only two state-of-the art review papers were found on the strengthening of concrete structures using TRM composites [37,38]. In the first paper, Awani et al. [37] presented a critical review of existing research on structural strengthening with TRM composites. In the second paper, Koutas et al. [38] described the tensile and bond behavior of TRM composites and included an overview of studies on the use of TRM for flexural, shear, confinement, and seismic retrofitting of concrete or RC members. A review paper on performance comparison of FRP versus TRM-strengthened RC structural members under ambient and high temperature environments could not be found.

This paper presents a critical overview of reported research on comparison between organic and inorganic matrix composites employed for the retrofitting of structural concrete members, identifies gaps in current knowledge, and summarises directions for future research. Section 2 of this paper presents in brief material characterization in terms of constituents and stress-strain behavior in tension, and also describes concisely methods of installation for both organic and inorganic composite systems. Sections 3 and 4 summarize available literature on bond behavior at composites-to-concrete interface at ambient and elevated temperatures, respectively. Section 5 enlists available research on use of organic versus inorganic matrix composites in flexural strengthening of RC beams. Research on effectiveness of TRM versus FRP composites in shear strengthening of RC beams is summarized in Section 6 with discussion of main findings. A review of available design guidelines and code provisions for both FRP and TRM composite systems for strengthening RC structures is briefly mentioned in Section 7. Conclusions and recommendations for future research are outlined in Section 8.

2. Material characterization and methods of installation

This section describes characterization of organic and inorganic composites in terms of constituent materials and stress-strain behavior in tension. It also covers methods used for composite system installation on concrete members. It should be noted that as for FRP composites material characterization is well documented in the literature and given in details elsewhere [39], it is briefly outlined herein. However, due to the relatively recent use of TRM composites, material characterization is given in details for inorganic matrix composites.

2.1. FRP composites

Fiber reinforced polymer (FRP) composites have achieved worldwide recognition as structural materials mainly because of numerous advantages [39–41]. Although these materials are in use since 1970s, substantial research devoted over past few decades has resulted in its popular use, especially in enhancing the capability of structural members [42–47]. The fibers which have gained the interest of the construction industry are glass, carbon, and aramid (Fig. 2). The mechanical properties of these fibers of the same type may differ considerably from one manufacturer to the other [39,40,45]. On the other hand, the binder is organic thermosetting polymers such as epoxy, polyester, polyurethane, vinylester, or phenolics. After polymer impregnation in fibers and subsequent setting/hardening, the composite so produced acts as a combined system and the stresses are transferred through bond at the interface of the two materials. The standard FRP coupons are tested as per ASTM D3039/3039 M [48] for establishing the mechanical properties of the resulting FRP system. Fig. 3 shows the overall stress-strain variation for average FRP systems against the conventional material, i.e. steel. The FRP systems exhibit linear-elastic response unlike the elasto-plastic response of steel. More details about material characterization of FRP composites can be found elsewhere [39,49,50].

All substrates for implementing the retrofitting system should be dried out, as required by the manufacturer. Before the application of FRP systems, surface preparation is usually required in terms of sandblasting, brushing, and cleaning to prepare substrate for the bonding of the system. There are three primary methods for installation of FRP systems onto concrete members: hand layup, machine wraps, and pre-cured systems (see Fig. 4).

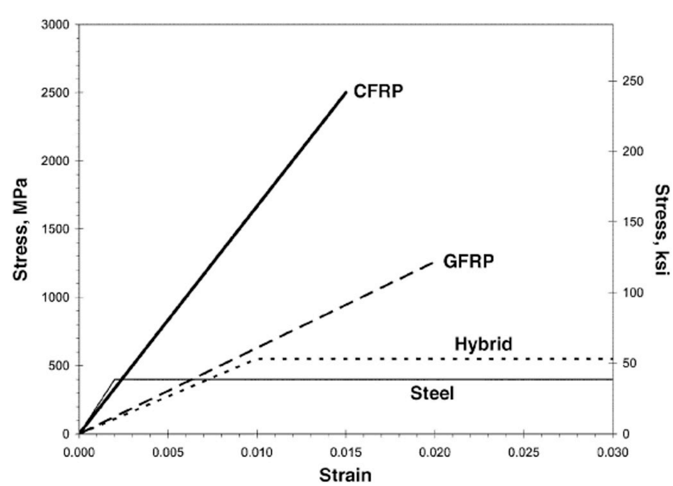

Fig. 3. Typical stress-strain curves for FRP composites [39].

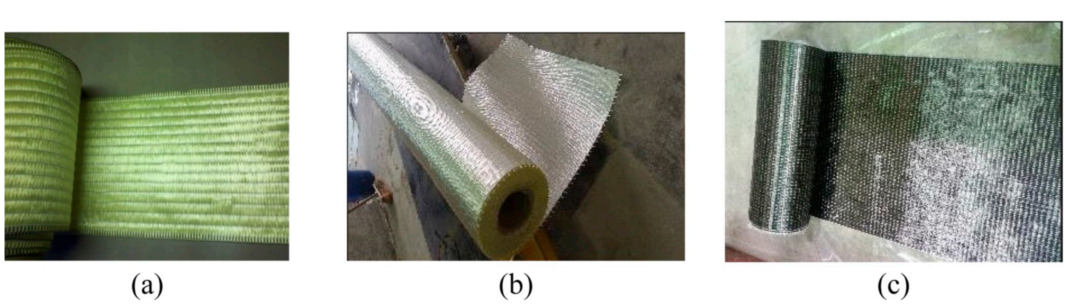

Fig. 2. Types of fibers used in FRP composites: (a) Aramid; (b) Glass; (c) Carbon.

(a) (b) (c)

Fig. 4. Installation methods for FRP systems: (a) Hand layup [50]; (b) Machine wrap [50]; (c) Pre-cured systems [51,52].

2.2. TRM composites

TRM composites have been widely recommended as a feasible substitute for the FRP systems for the retrofitting of RC structural members. The research on TRM started in 1980's, however, it was at a slow pace till the late 1990's and picked up from 2002 [31,53–55]. The method of its application on structures being similar to FRP composites, TRM composites overcome many drawbacks of FRP composites. However, unlike the use of polymer resin in FRP, the cementitious mortar lacks the capability to impregnate the fibers for holding them together [28,46,56–59]. This resulted in the substitution of fiber sheets with fiber textiles/fabrics having open meshes for enabling a mechanical interlock between cementitious mortar and the fibers [31].

2.2.1. Fabrics and textiles

As stated earlier, TRM is comparable to the FRP and may also be called as the "twin brother" [60]. Sometimes, smaller amount of epoxy is used as a coating on fiber strands for improving the durability or making the manufacturing and handling easier, however, it generally does not properly impregnate the fibers, thus the use of dry fabric is valid [31,43,44,46,58,61,62]. The common fiber materials are basalt, glass, carbon, polyphenylene benzobisoxazole (PBO), and aramid (Fig. 5). These fiber materials are recognized for having low processing costs, high strength-to-weight ratio, and improved corrosion and fatigue resistance because of their composite action [63]. The glass being prone to alkali corrosion, the use of ordinary glass in the highly alkaline cementitious mortar is not recommended. Therefore, alkali-resistant (AR) glass is used in TRM applications [64]. Test coupons of the textiles are tested in uniaxial tension for establishing their mechanical properties, as seen in Fig. 6 [58].

2.2.2. Mortars

The cementitious mortar used in TRM composites plays an important role as it acts as a medium for the transfer of the applied force to the strong textile after its impregnation. The general required characteristics of the mortar are: non-shrinkability, good workability so that it can be applied using a trowel, high viscosity (required for overhead or vertical surfaces), lesser rate of loss of workability (for successive application of layers) and strong shear resistance for avoiding early debonding [65]. This inorganic matrix can be either cementitious mortars or polymer modified cementitious mortars [58]. In both types, Portland cement is usually used with the addition of a low dosage of dry polymers at less than 5% by weight of cement in the second type. The use of polymers improves the bond between mortar and fibers, makes the workability

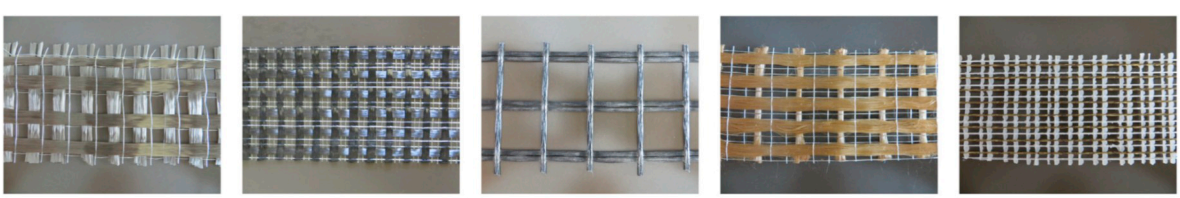

(a) (b) (c) (d) (e)

Fig. 5. Fabric materials used in TRM composites [2]: (a) Basalt; (b) Carbon; (c) Glass; (d) PBO.

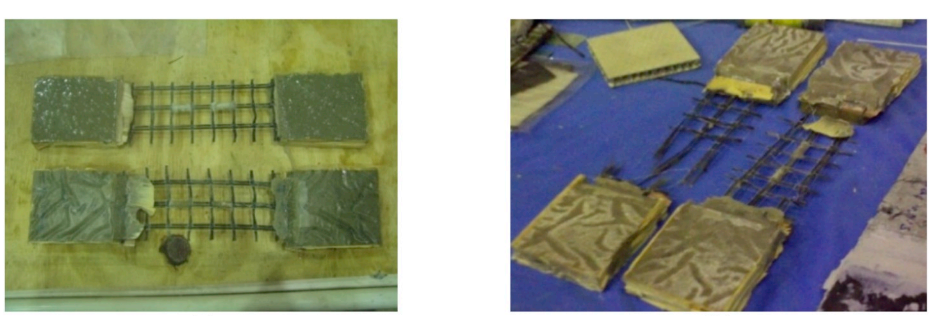

(a) (b)

Fig. 6. Bare textile coupons [58]: (a) Before testing; (b) After testing.

and setting time appropriate for this application, and enhances the shear strength of mortar [31,66]. The quality of matrix depends upon the strength of bond that the mortar forms with fabric, and the substrate, which cannot be accurately assessed from the mechanical properties of mortar. Based on the fabric being used, cementitious mortar can be optimized by using adhesion promoter, cement of higher fineness, additives, fly ash, micro aggregates, and inorganic nanoparticles [31,66]. The compressive strength of mortar is determined using 50-mm mortar cubes, which are tested as per ASTM C109/C109 M [67], as seen in Fig. 7 (a). For measuring the tensile strength of mortar, briquette specimens are prepared and tested in accordance with ASTM C190 [68], as seen in Fig. 7(b).

2.2.3. Composite properties

Many researchers have studied the tension behavior of TRM composites. The ICC Evaluation Service has provided the testing standard for establishing the tensile properties of TRM composites [61]. The test requires casting a single or multiple layers of TRM in a large wooden form. The response of the TRM system is a function of both constituent materials (bare textile and mortar) as well as the gripping method adopted in the test.

There are three distinct regions in the non-linear stress-strain variation, as seen in Fig. 8. Initially in Stage I, the cementitious mortar is intact with no cracks and thus contributes significantly to the load as well as the stiffness of the TRM composite. The Stage II is characterized by the initiation of cracks in mortar that grow progressively. The development of cracks is responsible for the drop in load and the stress-strain curve becomes uneven. The Stage III starts when the mortar gets completely cracked and subsequent increase in displacement causes linear increase in stress, as the load is carried by the fibers alone. The existing cracks in mortar get widened in this stage. Stage III ends when fibers fracture i.e. the strain is equal to the fracture strain of fibers.

Fig. 7. Standard testing of mortar specimens [69]: (a) Cube specimens in compression; (b) Briquette specimens in tension.

2.2.4. Method of installation

Before the installation of TRM systems, surface preparation is required in terms of sandblasting, brushing, and cleaning to make the substrate suitable for developing bond with mortar. After cleaning and dampening the concrete surface, a layer of mortar about 2 mm thick is applied on the prepared concrete surface using a metal trowel. The fiber textile is then placed and pressed lightly into the cementitious mortar so that the mortar protrudes from the fiber textile mesh openings. The next mortar coating is then applied so as to fully cover the textile fabric. This procedure is repeated for every subsequent TRM layer. A final mortar coat of about 3 mm thickness is applied and the surface is levelled using trowel. The mortar of the previous layer should be wet before applying the next layer of mortar. Thus the delay between the laying of the two consecutive layers of mortar is very crucial. These steps are shown in Fig. 9.

3. Bond behavior of FRP and TRM composites at ambient temperature

This section covers main aspects related to bond behavior of FRP and TRM composites at room temperature in terms of failure modes and bond-slip models.

3.1. FRP composites

The bond between the FRP laminates and concrete plays a major role in transferring shear stresses from the parent RC structural member to the FRP laminates for both flexural and shear strengthening cases. Different test methods have been developed for the characterization of the local behavior of the interfacial shear bond [33]. These methods include single/double shear lap tests, bending test, mixed-mode test, and direct tension pull-off test (Fig. 10).

The examined interfacial bond characteristics cover the bond stress-slip relationship, effective bond length, average shear bond strength, maximum shear bond stress, and interfacial fracture energy. The pull tests clearly show that in almost all of the cases (with the exception of systems using high concrete strength or weak adhesive) the failure of FRP-concrete bond is by the spalling of concrete cover (see Fig. 11).

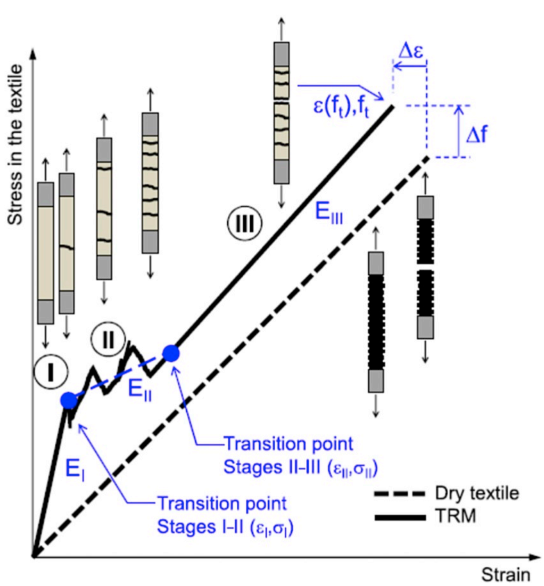

Fig. 8. TRM tensile response stages [70].

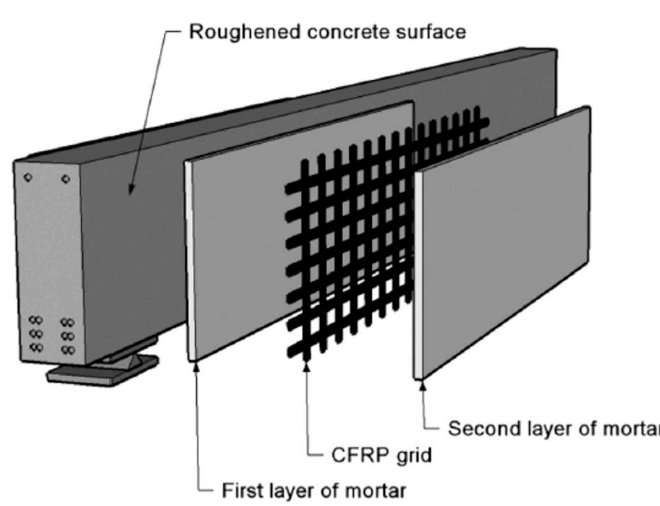

Fig. 9. TRM strengthening system [71].

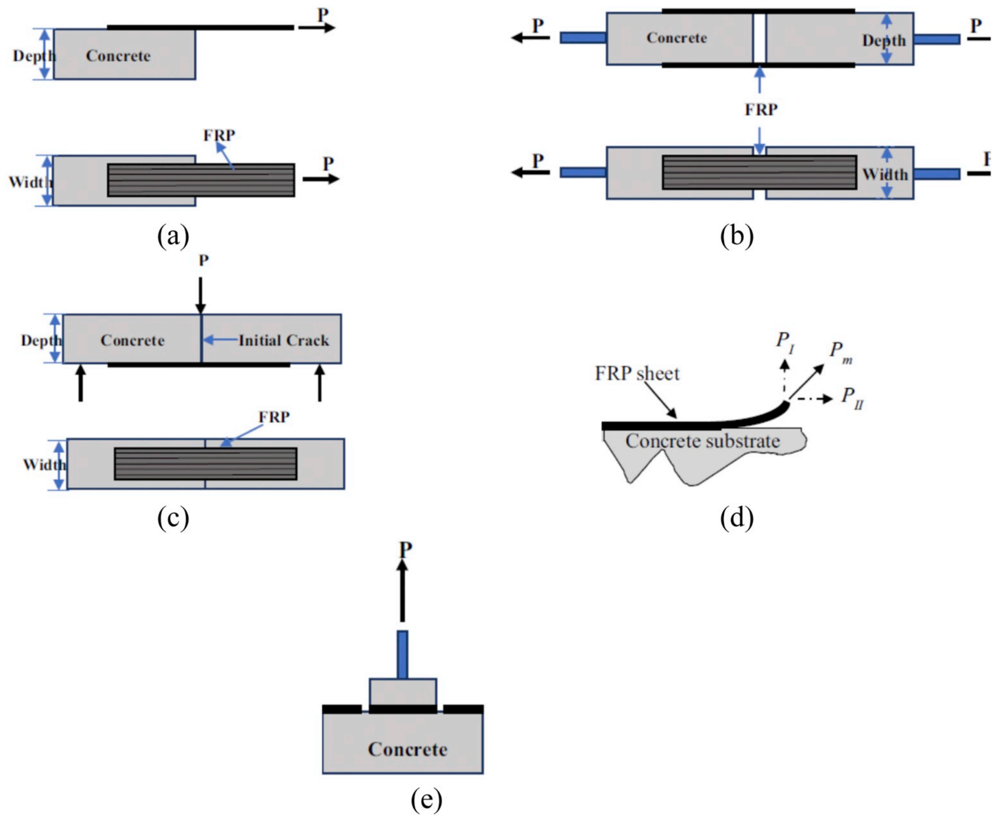

Fig. 10. Major classifications of FRP-concrete test methods [33]: (a) Single shear lap test; (b) Double shear lap test; (c) Bending type test; (d) Mixed-mode type test; (e) Direct tension pull-off test.

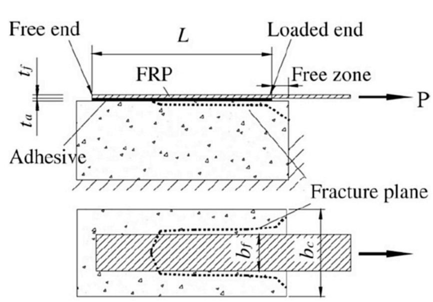

Fig. 11. Failure mode at FRP-concrete interface in a pull test [72].

3.1.1. Bond-slip models

The most popular method of representing the FRP-concrete bond behavior is through the construction of bond-slip curve (Fig. 12). The area under the bond-slip curve provides an estimate for the fracture energy (G_f -mode) [73]. The bond-slip models available in literature were summarized in the papers by: Ko et al. [74], Lu et al. [72], and Sayed-Ahmed et al. [75]. Table 1 lists existing bond-slip models at FRP-concrete interface. Out of all available bond-slip models, the simplified model proposed by Lu et al. [72] has been successfully used in the literature for calibration of finite element modeling against experimental data of FRP-strengthened RC beams and slabs [58,76,77].

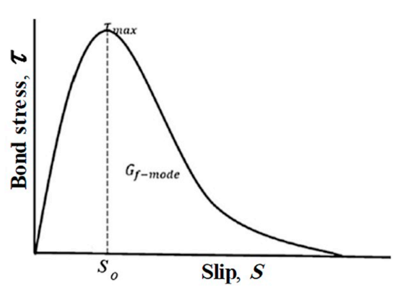

Fig. 12. Typical bond-slip curve at FRP-concrete interface [33].

3.2. TRM composites

Bond behavior of TRM composites has been recently studied in the literature [85–87] and the outcome of these studies is discussed in the subsequent text. The test methods frequently used for investigating the bond behavior of TRM composites are single-lap (Fig. 13(a)) and double-lap (Fig. 13(b)) shear tests [87–90].

The most common mode of bond failure in TRM composites is the debonding at the fabric-matrix interface. It is caused by the formation of transverse cracks, which originate from a horizontal crack formed at the interface of concrete and fabric-matrix (Fig. 14). The debonding mode of failure of fabric-matrix is followed by slip and deformation of longitudinal fibers [85,90,91]. This mode of failure was clearly seen in tests reported by Sneed et al. [90], wherein the longitudinal fibers are pulled from the cementitious matrix.

The bond failure of TRM composite, in some instances, is mainly caused by slipping of the textile, which has been observed by Ombres [87] in the tests involving one TRM layer. Based on the type of mortar matrix employed, inconsistencies were observed in the textile-matrix bond with concrete, which were the cause of debonding of TRM composite from the concrete [87]. This illustrates the need for the surface preparation before the bonding of the TRM composite.

Although rare, the rupture of textile is also reported in the literature. Awani et al. [85] reported the rupture of fibers in specimens tested under cyclic loads, which were retrofitted using a matrix that displayed

Table 1
Existing bond-slip models at FRP-concrete interface[a].

Bond-slip model	Ascending branch $s \le s_o$	Descending branch $s > s_o$	$\tau_{\max}$	s_o	s_f	β_w	Notes
Brosens and Van Gemert [78]	$\tau = \tau_{\max}\left(\frac{s}{s_o}\right)$	$\tau = \tau_{\max}\left(\frac{s_f - s}{s_f - s_o}\right)$	$1.8\beta_w f_t$	$2.5\tau_{\max}\left(\frac{t_a}{E_a} + \frac{50}{E_c}\right)$	$\frac{2G_f}{\tau_{\max}}$	$\sqrt{\frac{1.5\left(2 - \frac{b_f}{b_c}\right)}{1 + \frac{b_f}{100}}}$	Bilinear curve $G_f = 0.3 f_t \beta_w^2$
Neubauer and Rostasy [79]	$\tau = \tau_{\max}\left(\frac{s}{s_o}\right)$	$\tau = 0$	$1.8 f_t$	$0.224\beta_w^2$	–	$\sqrt{\frac{1.06\left(2 - \frac{b_f}{b_c}\right)}{1 + \frac{b_f}{400}}}$	A linear ascending branch and a sudden drop
Monti et al. [80]	$\tau = \tau_{\max}\left(\frac{s}{s_o}\right)$	$\tau = \tau_{\max}\left(\frac{s_f - s}{s_f - s_o}\right)$	$1.8\beta_w f_t$	$2.5\tau_{\max}\left(\frac{t_a}{E_a} + \frac{50}{E_c}\right)$	$0.33\beta_w$	$\sqrt{\frac{1.5\left(2 - \frac{b_f}{b_c}\right)}{1 + \frac{b_f}{100}}}$	Bilinear curve
Nakaba et al. [81]	$\tau = \tau_{\max}\left(\frac{s}{s_o}\right)\left[\frac{3}{2 + \left(\frac{s}{s_o}\right)^3}\right]$		$3.5 f_c^{'0.19}$	0.065	–	–	A single curve
Savioa et al. [82]	$\tau = \tau_{\max}\left(\frac{s}{s_o}\right)\left[\frac{2.86}{1.86 + \left(\frac{s}{s_o}\right)^{2.86}}\right]$		$3.5 f_c^{'0.19}$	0.051	–	–	A single curve
Dai and Ueda [83]	$\tau = \tau_{\max}\left(\frac{s}{s_o}\right)^{0.575}$	$\tau = \tau_{\max} e^{-\beta(s - s_o)}$	$\frac{-1.575\alpha K_a + \sqrt{2.481\alpha^2 K_a^2 + 6.3\alpha\beta^2 K_a G_f}}{2\beta}$	$\frac{\tau_{\max}}{\alpha K_a}$	–	–	$\alpha = 0.028\left(\frac{E_f t_f}{1000}\right)^{0.254}$ $\beta = 0.0035 K_a\left(\frac{E_f t_f}{1000}\right)^{0.34}$ $G_f = 7.554 K_a^{-0.449}(f_c^{'})^{0.343}$ $K_a = \frac{G_a}{t_a}$
Dai et al. [84]	$\tau = 2BG_f(e^{-Bs} - e^{-2Bs})$		$0.5BG_f$	$0.693B$	–	–	A single curve $B = 6.846(E_f t_f)^{0.108}\left(\frac{G_a}{t_a}\right)^{0.833}$ $G_f = 0.446(E_f t_f)^{0.023}(G_a/t_a)^{-0.352}(f_c^{'})^{0.236}$
Lu et al. [72]	$\tau = \tau_{\max}\sqrt{\frac{s}{s_o}}$	$\tau = \tau_{\max} e^{-\alpha\left(\frac{s}{s_o} - 1\right)}$	$\tau_{\max} = 1.5\beta_w f_t$	$s_o = 0.0195\beta_w f_t$	–	$\sqrt{\frac{2.25 - b_f/b_c}{1.25 + b_f/b_c}}$	$G_f = 0.308\beta_w^2\sqrt{f_t}$ $\alpha = \frac{1}{\frac{G_f}{\tau_{\max} s_o} - \frac{2}{3}}$
Ko et al. [74]	$\tau = \tau_{\max}\left(\frac{s}{s_o}\right)$	$\tau = \tau_{\max} - \frac{\tau_{\max}(s - s_o)}{(s_f - s_o)}$	$0.165 f_c^{'}$	$-0.001 f_c^{'} + 0.122$	$-0.002 f_c^{'} + 0.302$	–	Bilinear curve

[a] All units are: N and mm; B = interfacial parameter; b_c = width of concrete member; b_f = width of FRP sheet; E_a = elastic modulus of adhesive; E_c = elastic modulus of concrete; E_f = elastic modulus of FRP; $f_c^{'}$ = concrete compressive cylinder strength; f_t = concrete tensile strength; G_a = elastic shear modulus of adhesive; G_f = interfacial fracture energy; K_a = shear stiffness of adhesive layer; s = local slip; s_o = local slip at maximum bond stress $\tau_{\max}$; s_f = local slip when local bond stress reduces to zero (maximum slip); t_a = thickness of adhesive layer; t_f = thickness of FRP; β_w = width ratio factor; τ = local bond stress; $\tau_{\max}$ = maximum local bond stress.

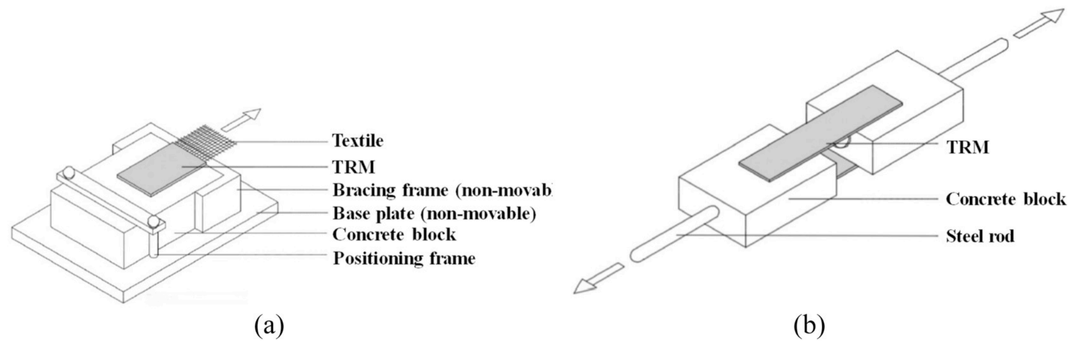

Fig. 13. TRM-to-concrete test methods [37]: (a) Single shear lap test; (b) Double shear lap test.

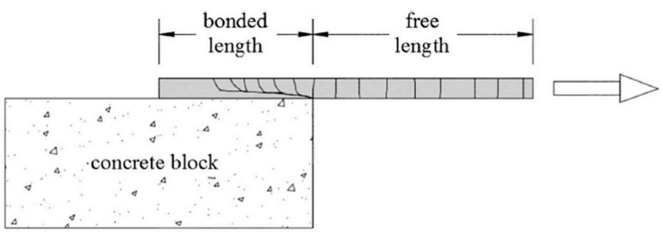

Fig. 14. Typical bond failure at fabric-matrix interface for TRM composites [85].

irregular bond response with the textile. It was thought that the textile was damaged because of the repeated grinding of fibers with the matrix during the cyclic loading.

In a recent study by Raoof et al. [92], bond at TRM-concrete interface has been investigated for different bond lengths and different number of TRM layers varying from 1 to 4. It was found out that the failure mode is related to the number of TRM layers. Specifically, specimens retrofitted with one or two layers of TRM composite failed by the slipping of the fabric from the mortar, while specimens having 3 or 4 layers of TRM composite failed because of the debonding of TRM from the concrete, which caused the spalling of concrete cover. This was a new finding as all previous studies on TRM bond behavior had reported the occurrence of failure either at the mortar-concrete interface without affecting the concrete cover or at the mortar-fabric interface. This was mainly because of using a maximum of two layers of TRM in these tests. Tetta et al. [93] has also reported the peeling (or spalling) of concrete cover in their study involving the shear strengthening of RC beams using U-jackets of TRM composite. Raoof [94] also observed the peeling of concrete cover in RC beams, which were strengthened in flexure using TRM composite. The occurrence of this type of failure, which is common in FRP-strengthened RC members [95], indicates that the TRM composite can perform similar to FRP composite. In conclusion, the different TRM-to-concrete failure modes reported in the literature are summarized in Fig. 15.

3.2.1. Bond-slip models

A typical bond-slip curve of TRM specimens is similar to FRP-concrete interface shown previously in Fig. 12. Bond-slip models for bond at TRM-concrete interface are very limited in the literature. To date, only few models have been found [86,87,97]. The models presented by D'Ambrisi et al. [86] and Ombres [87] give equations for the whole bond-slip curve. However, Jung et al. [97] presents only an equation for the calculation of stresses in the TRM composite at debonding. The model of Ombres [87] is explained as follows:

Bond stress at any slip (s) is given by.

$$\tau(s) = [\tau_o + A(e^{-\alpha s} - e^{-\beta s})]\left(1 - \frac{s}{s_f}\right) \qquad 0 \le s \le s_f \tag{1}$$

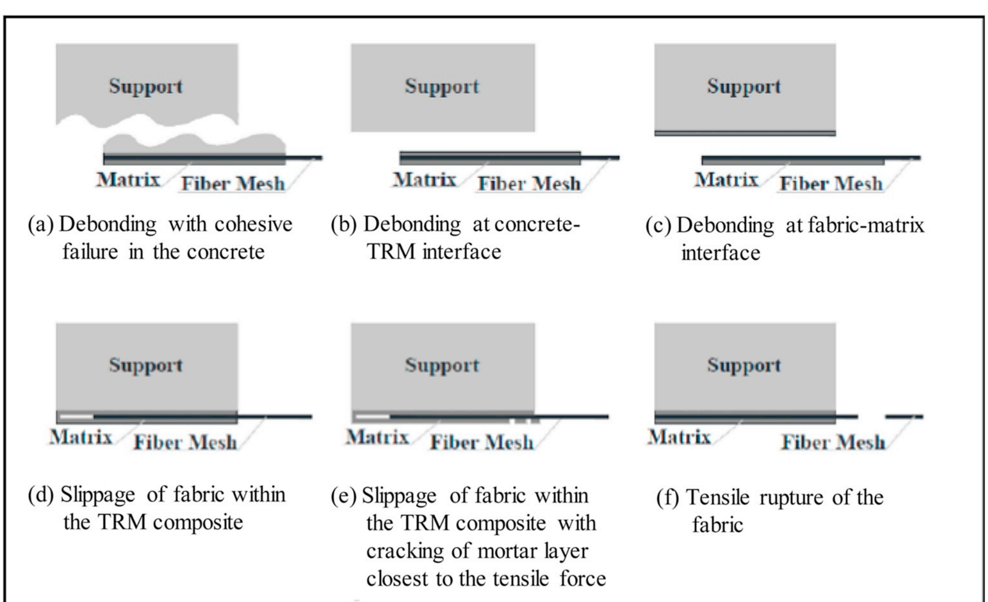

Fig. 15. Different failure mechanisms at TRM-concrete interface [96].

Table 2
Parameters of the bond-slip model of Ombres [87].

Parameter	Value
τ_o (MPa)	0.150
A	0.700
α	0.005
β	6.000
s_f (mm)	0.650

where τ_o = initial finite value of bond shear stress; s_f = final slip when value of bond stress is zero; and A, α and β are curve-fitting parameters. All parameters related to the above equation are given in Table 2.

4. Bond behavior of FRP and TRM composites at elevated temperature

4.1. FRP composites

There are limited studies addressing the bond behavior of FRP-concrete interface at elevated temperatures [98–104]. Many researchers [98,101,102,104] conducted double lap shear tests at temperatures ranging from low temperatures (10 °C–20 °C) to temperatures (70 °C–90 °C) higher than the T_g level of resin used for externally bonding CFRP strips to concrete. At temperatures below the T_g level, the bond strength increased by 10%–41%. Whereas, at temperature above T_g level, there was reduction in bond strength (18%–60%). Low T_g resin showed greater reduction in strength when exposed to temperature higher than the T_g level [104]. The mode of failure was cohesive or mixed cohesive-adhesive failure at ambient temperature and adhesive at elevated temperature.

Gamage et al. [100] conducted single lap shear tests on concrete bonded with CFRP sheets using resin (T_g not reported). The test results showed similar trend as that of Wu et al. [104]; the bond strength reduced with increase in temperature and the drop in strength was steep in the range of 50–75 °C after which the normalized bond strength was reduced by more than 75%. Up to 50 °C, the mode of failure was a combination of bond failure and concrete rupture, and for temperatures above 60 °C, the failure occurred by peeling-off adhesive.

Leone et al. [103] conducted double lap shear tests at temperatures of 20 °C–80 °C on concrete externally bonded with CFRP sheets or strips using resin having T_g of 55 °C. For the CFRP strips, the bond strength decreased (−15%) for temperature below T_g (50 °C) and increased (+9%) for temperature above T_g. For CFRP sheets, the bond strength increased up to 65 °C (24% at 50 °C and 7% at 65 °C); however, at higher temperature of 80 °C, there was a reduction of 11%. These results (except the CFRP sheet results at 80 °C) were in contrast to those reported by Blontrock [98], Klamer et al. [102] and Klamer [101].

Recently, Firmo et al. [99] conductred double lap shear tests at elevated temperatures of 20 °C–120 °C on concrete externaly bonded with CFRP strips using resin having a T_g of 47 °C. It was reported that the increase in temperature causes (i) reduction in bond strength, (ii) softening of epoxy leading to much more linear axial interfacial strain distribution, and (iii) shifting in the mode of failure from cohesive to adhesive (Fig. 16). The temperature dependent bond-slip relations were developed. There was considearble reduction in maximum shear stress and stiffness at elevated temperature. The steady state and transient conditions caused similar reductions in bond strength with a loss of about 77% at 120 °C.

The review of studies presented above indicates that the elevated temperature affects the bond performance of CFRP-concrete interfaces. The above studies are contradictory on the effect of temperature on bond strength, especially when the temperature is below T_g. For exposure to a temparature less than T_g, some studies show increase in bond strength, whereas other studies show reduction in bond strength. Fig. 17 summarises the test reults of these studies. Other than this issue, the results are broadly similar.

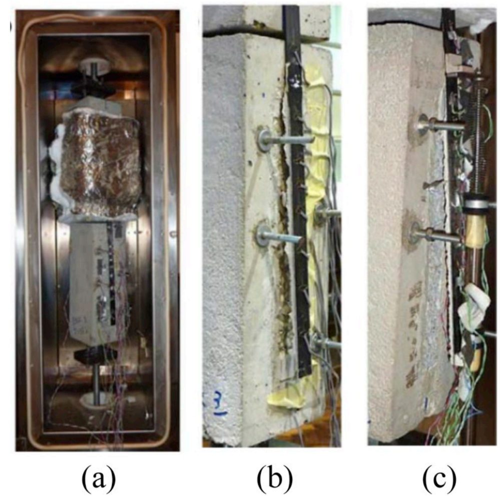

Fig. 16. Double lap shear tests conducted on CFRP-strngthened concrete blocks by Firmo et al. [99]: a) General view of tests; (b) Failure mode at ambient temperature (cohesive failure); (c) Failure mode at high temperature exposure (adhesive failure).

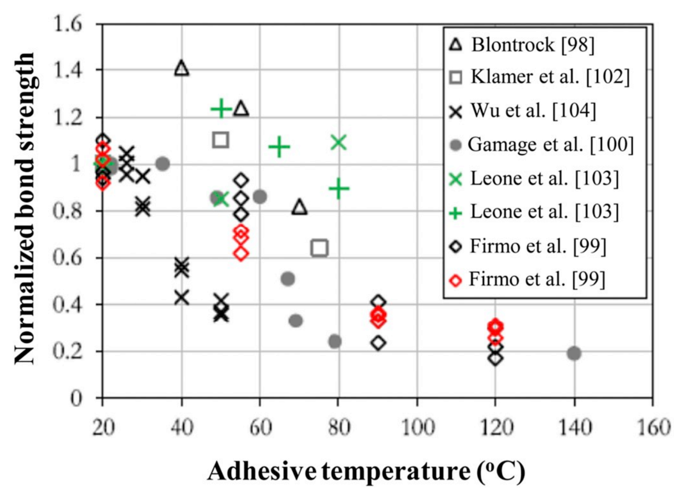

Fig. 17. Normalized bond strength at FRP-concrete interface as a function of adhesive temperature [99].

4.2. TRM composites

The qualities that make the TRM composites outperform FRP composites at elevated temperatures due to the use of cementitious mortar as binding agent are: non-combustibility, non-flammability, and breathability. Although the bond behavior of TRM composites at ambient temperature has been extensively studied, there are limited studies in the literature for studying the bond performance of TRM composites at elevated temperature (e.g. Ref. [105]) due to which the comparison of its performance with FRP composites at elevated temperature is rare.

A recent paper by Raoof and Bournas [105] has examined the bond performance of TRM composites with concrete at elevated temperatures and compared its performance with FRP composites. The carbon fibers used in the two composites were the same. FRP composites were exposed to temperatures ranging from 20 to 150 °C, whereas, the TRM composites were exposed to higher temperature range of 20–500 °C. The number of layers were 3 or 4 in both the systems. Out of a total of 68 double-lap shear test specimens, 56 were tested at steady state and the remaining at

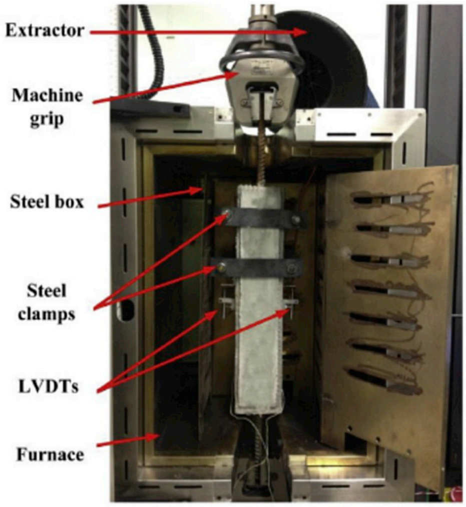

Fig. 18. Test setup for the mortar prisms tested at high temperature in the study of Raoof and Bournas [105].

transient state. The test setup is shown in Fig. 18. At low temperature of 20 °C, the bond performance of FRP was superior to TRM with the bond strength of 3 and 4 layers of FRP being 140% and 150% higher than the corresponding specimens of TRM. Nevertheless, at elevated temperatures, the bond performance of TRM was much better than FRP. In steady-state tests, although the residual bond strength of FRP specimens at 150 °C was only 17%, the residual bond strength of TRM system at much higher temperature of 400 °C was 85%. As expected, FRP system exhibited premature adhesive bond failure at 150 °C.

4.3. FRP versus TRM composites in flexural strengthening of RC beams

There are limited studies that compare between FRP and TRM composites for upgrading the flexural strength of RC beams. These studies are summarized in the following section.

4.4. Summary of conducted research

Dated between 2001 and 2017, only few studies have been found in the literature concerning the comparison between organic and inorganic matrix composites in the flexural strengthening of concrete beams. First study was carried out by Kurtz and Balaguru [106], wherein RC beams, strengthened using carbon fiber sheets externally bonded with the help of inorganic binder, were tested in flexure. The test results of this study were compared with an earlier study, which differed only in the type of binder, which was organic. The test results showed that the increase in the strength and stiffness was at par with the organic matrix, but there was minor decrease in ductility. However, the mechanism of failure in inorganic matrix was sheet rupture, as against the sheet delamination observed in the organic matrix. The brittle nature of inorganic matrix was responsible for the change in failure mechanism.

Wu and Sun [107] compared the strengthening efficiency of cementitious and resin binders in flexural strengthening of RC beams. Resin and cementitious binders were used independently to prepare thin CFRP and carbon fiber reinforced cement (CFRC) sheets, which were employed to upgrade plain concrete beams for upgrading the flexural capacity. The unstrengthened plain concrete beam showed brittle behavior. However, both flexural strength and ductility of the CFRP-strengthened beam increased significantly. This beam failed due to debonding of the CFRP sheet from the concrete substrate followed by concrete crushing under the loading pin. The flexural strength of the CFRC-strengthened beam was much lower than that for the CFRP-upgraded beam and the final failure was due to rupture of the CFRC sheet in the maximum moment zone.

Papanicolaou et al. [108] investigated the performance of TRM in comparison with FRP for flexural strengthening of RC beams. Two RC beams were strengthened in flexure using 4 layers of carbon textile as reinforcement. The two beams differed in the use of binder: cementitious mortar (TRM-strengthened) was used in the first, whereas the epoxy resin (FRP-strengthened) was used in the second. The ultimate load of FRP-strengthened beam was 12.6% higher than the TRM-strengthened beam. The failure of FRP-strengthened beam was by tensile rupture of FRP, whereas TRM-strengthened beam failed by debonding of TRM at the end.

In another study by Toutanji and Deng [109], the effectiveness of RC beams retrofitted with carbon fiber laminates bonded using organic and inorganic binders was compared experimentally. Although the inorganic matrix was as effective as the organic matrix in enhancing the strength and stiffness of RC beams, the mechanism of failure of the inorganic matrix was more brittle. The test specimens of inorganic matrix failed through the formation of cracks in the composite with minimum accumulation of strain on the concrete-composite interface. However, the failure of RC beams retrofitted using the organic matrix was characterized by the delamination of the carbon laminates. For the beams with 3 and 4 layers of carbon fiber sheets, changing the matrix from organic to inorganic increased the post-crack flexural stiffness from 20 to 29%, kept the flexural capacity almost same, and reduced the deflection at ultimate load by about 8–9%. However, the beams with 2 layers of carbon fiber sheets, using inorganic binder instead of organic matrix decreased the post-crack stiffness, the flexural capacity and the deflection at ultimate load by about 13%, 20% and 31%, respectively.

Hashemi and Al-Mahaidi [110] compared experimentally the performance of one beam that was flexurally strengthened with two strips of carbon fabric attached to the bottom surface using normal epoxy adhesive with another beam in which cement-based mortar was used to attach two similar carbon fabric strips to the soffit. In both beams, the failure was characterized by a combination of mid-span and end debonding. As compared to the control, the ultimate load of the beam with organic matrix composites was 35% higher. However, in the beam with inorganic matrix composites, the ultimate load was 10% higher.

Elsanadedy et al. [58] investigated experimentally and numerically the effectiveness of externally bonded TRM in comparison with FRP

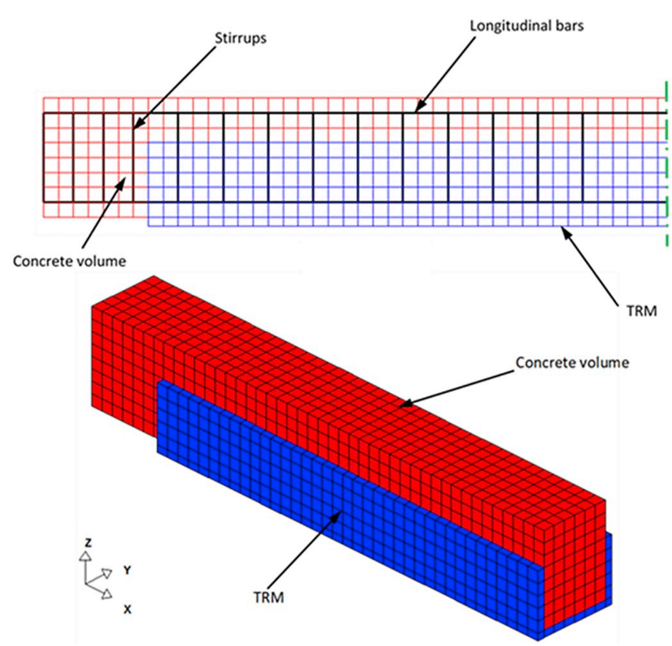

Fig. 19. Finite element mesh for half of TRM-strengthened beam tested by Elsanadedy et al. [58].

composites, as a means of increasing the flexural strength of RC beams. Two types of mortar namely, cementitious and its polymer modified version, were used. Three beams were strengthened using 5 or 10 layers of basalt-based textile reinforced inorganic mortar and one beam was retrofitted with one layer of carbon fiber/epoxy sheet. It is to be noted that the CFRP laminates were designed to provide almost same axial stiffness and strength of 5 layers of the bare textile. For the two TRM-retrofitted RC beams with equal number of TRM layers but different mortar types, the specimen with cementitious mortar failed abruptly because of the end debonding of TRM. However, at higher load, beam with polymer modified cementitious mortar failed as a result of the fabric rupture at mid-span. For the two counterparts (designed for same flexural strength), failure occurred because of textile and CFRP rupture at mid-span. Although both the FRP-strengthened and TRM-strengthened RC beams showed similar characteristics, they differed in: (i) ductility (TRM was 61% more effective in terms of deflection ductility), (ii) initiation of yielding (yielding in TRM initiated at a lower load), and (iii) ultimate load (flexural capacity of TRM specimen was 7.2% lower). The paper also presented results of nonlinear finite element (FE) analysis performed using LS-DYNA software [111]. FE model for half of one of the TRM-strengthened beams is shown in Fig. 19. The FE model was calibrated by the experimental data of this study and those by Papanicolaou et al. [108] and good agreement was found between experimental and numerical results as seen in Figs. 20 and 21.

In a recent research, Raoof et al. [112] compared the flexural behavior of concrete beams retrofitted using externally bonded layers of TRM and FRP composites having textiles of basalt, carbon, or glass fibers. The major findings reported in the paper are: (i) TRM was generally less effective than FRP in upgrading the flexural strength of concrete beams with the strength of TRM being 46%–80% of FRP; (ii) increasing the number of TRM layers from 1 to 3, flexural strength of TRM-upgraded beam rose from 47% to 80% of FRP; (iii) epoxy coating of carbon fiber fabric substantially improved the efficiency of TRM composite; coating one layer of textile with epoxy enhanced the flexural

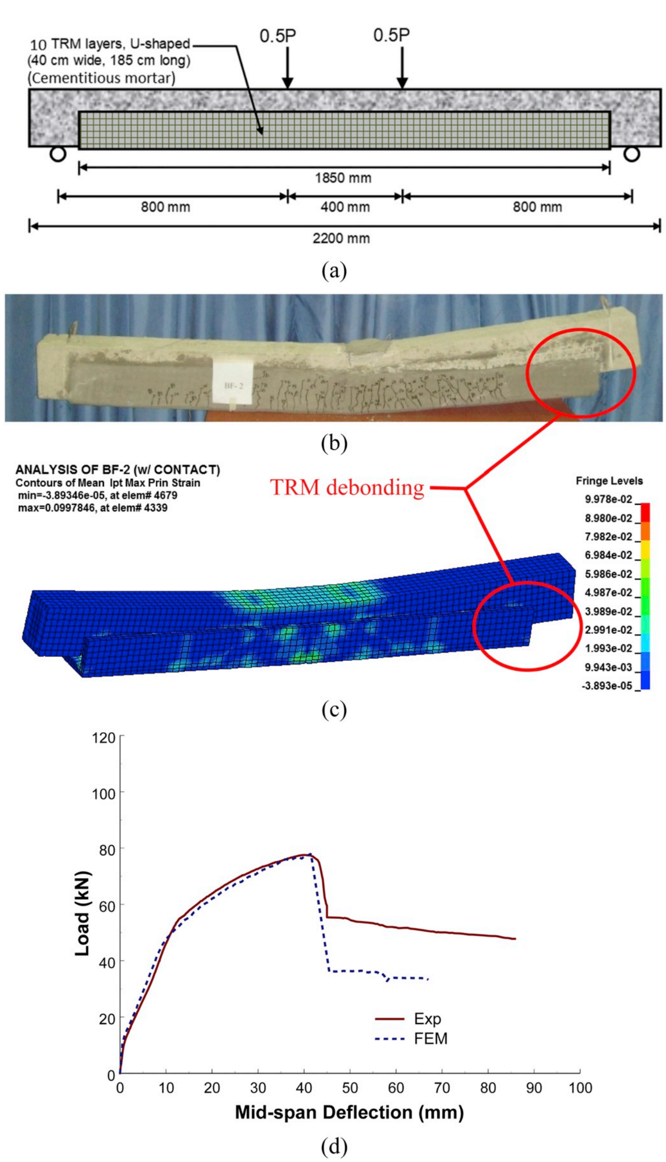

Fig. 20. Comparison of experimental and FE model results for TRM-strengthened beam with cementitious mortar tested by Elsanadedy et al. [58]: (a) Beam details; (b) Experimental mode of failure; (c) FE mode of failure; (d) Load-deflection curves.

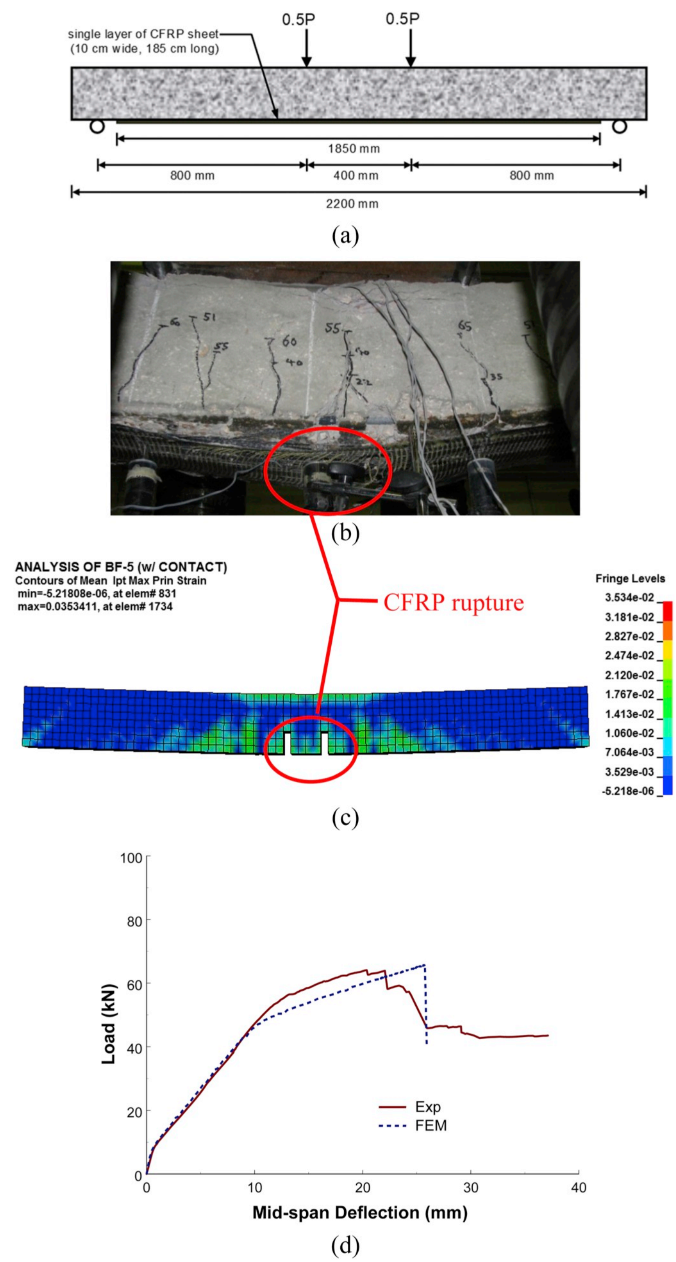

Fig. 21. Comparison of experimental and FE model results for CFRP-strengthened beam tested by Elsanadedy et al. [58]: (a) Beam details; (b) Experimental mode of failure; (c) FE mode of failure; (d) Load-deflection curves.

strength by 55%; (iv) the adoption of U-jacket for providing end-anchorage to FRP- and TRM-retrofitted RC beams caused 90% and 9% increase in the flexural strength respectively; the insignificant effect of end-anchorage in TRM system was due to the slipping of fabric from the anchorage because the U-jacket was not effective in anchoring the TRM layers; (v) there was considerable enhancement in the stiffness of strengthened beams of both systems; and (vi) textiles of different fiber materials but almost same axial stiffness led to different flexural strengths. The failure modes noticed in the FRP- and TRM-strengthened specimens are shown in Figs. 22 and 23 respectively. The modes of failure were affected by the number of TRM layers, the textile fiber materials, and the textile surface condition.

As a continuation of the previous study by Raoof et al. [112], Raoof and Bournas [113] compared experimentally the flexural behavior of RC beams retrofitted using FRP and TRM systems having carbon, basalt or glass fibers (uncoated and coated) at high temperature. Twenty-three half-scale strengthened RC beams were tested in flexure under four-point bending at a temperature of 150 °C (while hot) using the especially designed heating system. As expected, TRM exhibited better performance than FRP with TRM retaining 54% flexural strength, whereas FRP fully lost its strength. The increase in the number of layers of strengthening material increased the flexural strength in TRM system but there was negligible effect in FRP system because of the premature failure of epoxy. The epoxy coating of carbon fibers enhanced the flexural strength of TRM-strengthened beams. The adoption of end-anchorage in FRP system, increased the effectiveness of the strengthening system substantially at high temperature (11.4 times), which is attributed to the development of cold anchorage zones (see Fig. 24(a)). However, the corresponding increase for the TRM system was only 1.14 times, which was mainly because of the slipping of the fabric from the anchorage provided by U-jacket. The modes of failure noticed in the TRM system were: slipping of fibers, shearing between the layer of TRM, and debonding of TRM with or without peeling off concrete cover. However, FRP-retrofitted beams (except for FRP-strengthened beam with end anchorage) failed by adhesive failure (see Fig. 24(b)).

4.5. Discussion of main findings

4.5.1. Beams tested at ambient temperature

In order to compare the performance of FRP and TRM-strengthened beams tested in the previous studies, TRM versus FRP effectiveness ratio as first introduced by Raoof et al. [112] was estimated for TRM-strengthened beams and their FRP-upgraded counterparts tested by: Wu and Sun [107], Papanicolaou et al. [108], Toutanji and Deng [109], Hashemi and Al-Mahaidi [110], Elsanadedy et al. [58] and Raoof

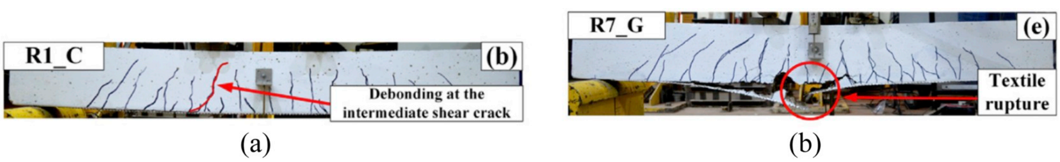

Fig. 22. Failure modes for representative FRP-strengthened beams tested by Raoof et al. [112].

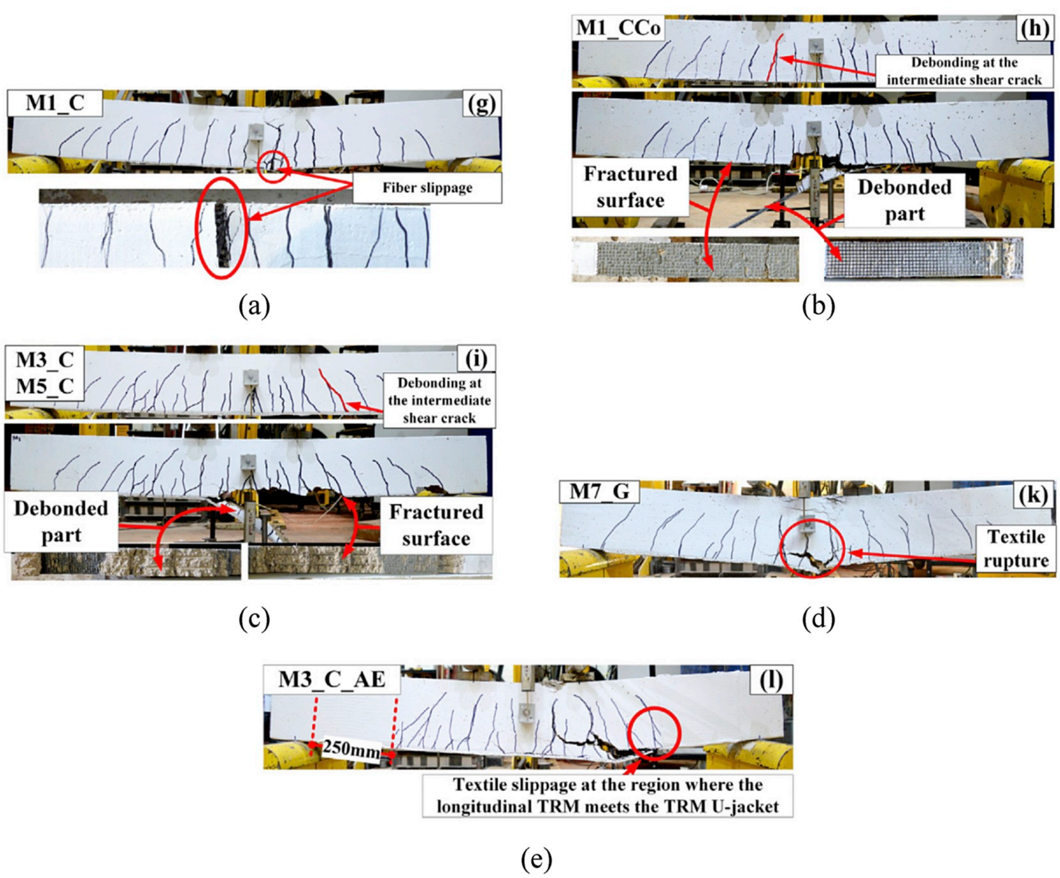

Fig. 23. Failure modes for representative TRM-strengthened beams tested by Raoof et al. [112].

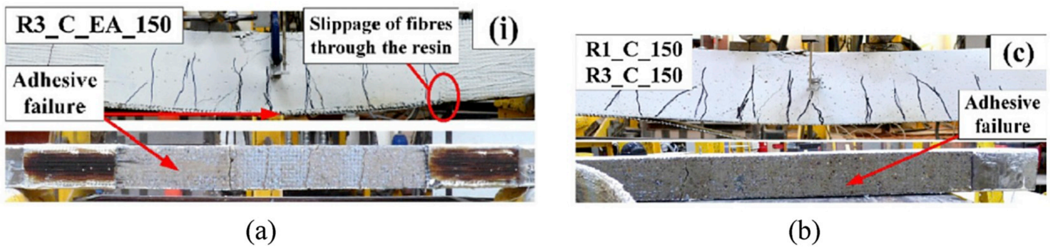

Fig. 24. Failure modes for representative FRP-strengthened beams tested by Raoof and Bournas [113] at high temperature: (a) Beam with end anchorage; (b) Beam without end anchorage.

et al. [112]. This effectiveness ratio is estimated from

$$\text{TRM versus FRP effectiveness ratio} = \frac{P_{u,TRM} - P_{u,co}}{P_{u,FRP} - P_{u,co}} \quad (2)$$

where $P_{u,TRM}$ = ultimate load for TRM-strengthened beam; $P_{u,co}$ = ultimate load for control unstrengthened beam; and $P_{u,FRP}$ = ultimate load for FRP-strengthened counterpart. These ratios are enlisted in Table 3 for 12 beams. From the table, it is clear that TRM was generally inferior to FRP in upgrading the flexural strength of RC beams, with the effectiveness ratio between the two systems varying from 0.27 to 1.0 with an average value of 0.65. However, for ultimate deflection comparison, FRP was a little better in enhancing the deflection capacity and hence ductility, with an average value of 0.91 for TRM to FRP ultimate deflection ratio as seen in Table 3. It is generally found out that TRM effectiveness is mostly affected by type of mortar selected, coating of textile material and number of TRM layers. Using polymer modified cementitious mortars gave better results than conventional cementitious mortar as noticed by Elsanadedy et al. [58]. Coating the dry textile fibers with epoxy adhesive significantly enhanced the performance of TRM material as clarified by Raoof et al. [112]. Also, TRM effectiveness was sensitive to the number of layers. It was found by Raoof et al. [112] that the TRM effectiveness ratio increased from 0.47 to 0.80 when the number of TRM layers increased from 1 to 3. From Table 3, it is noticed that the least TRM versus FRP effectiveness ratio was given by beams upgraded with one and two TRM layers with minimum and average ratio of 0.27 and 0.37. However, the average TRM versus FRP effectiveness ratio for beams strengthened with three or more TRM layers was 0.74. It is therefore recommended to use at least three TRM layers for flexural strengthening of RC beams; however, for FRP composites, one layer could be used. It is clear from Table 3 that only three types of failure mode were observed in the FRP-strengthened beams; namely: debonding at end of FRP sheets which propagates to middle of beam, debonding in the middle portion of the beam which propagates to the beam end, and rupture of FRP in the maximum-moment zone. However, in TRM-upgraded beams, five different failure modes were identified: end debonding, slippage of the rovings through the surrounding cement mortar, interlaminar debonding, debonding of TRM from the concrete with peeling off parts of the concrete cover, and rupture of the textile fibers at the constant moment zone. These failure modes were affected by the number of TRM layers, the textile fiber material, and the condition of textile surface (uncoated or coated fibers).

4.5.2. Beams tested at high temperature

For the beams tested by Raoof and Bournas [113] at high temperature of 150 °C, TRM versus FRP effectiveness ratios were calculated using Eq. (2) and listed in Table 4. In addition, both TRM and FRP effectiveness ratios due to heating were assessed from

$$\textit{TRM (or FRP) effectiveness ratio due to heating} = \frac{P_{u,TRM,T} - P_{u,co,R}}{P_{u,TRM,R} - P_{u,co,R}} \quad (3)$$

where $P_{u,TRM,T}$ = ultimate load for TRM-strengthened beam at elevated temperature; $P_{u,co,R}$ = ultimate load for control unstrengthened beam at room (or ambient) temperature; and $P_{u,TRM,R}$ = ultimate load for TRM-strengthened beam at room (or ambient) temperature. These ratios are also enlisted in Table 4 for the ten beams tested by Raoof and Bournas [113]. It is noted that TRM displayed excellent behavior as a retrofitting material in enhancing the flexural strength at elevated temperatures. As compared to the performance at ambient temperature, TRM retained an average effectiveness of 54%. On the contrary, FRP lost most of its effectiveness at elevated temperature, as seen in Table 4. TRM versus FRP had an average effectiveness ratio of 2.92 at elevated temperature of 150 °C, whereas the same ratio was 0.62 at ambient temperature (see Table 3). It is also noted from Table 4 that the TRM versus FRP effectiveness ratio decreased dramatically for specimens with end anchorage in which FRP had better performance due to the effect of the cold anchorage zones.

5. FRP versus TRM composites in shear strengthening of RC beams

There are limited studies showing comparison between TRM and FRP composites in enhancing the shear strength of RC beams. These studies have been summarized below.

5.1. Summary of conducted research

Wiberg [114] conducted large-scale tests on RC beams strengthened in shear with externally bonded carbon fiber sheets in a polymer-modified cementitious matrix. Six beams were tested which included two control beams without and with shear reinforcement, three beams strengthened in shear with one layer of carbon fiber sheet bonded with polymer-modified cementitious mortar (one without internal shear reinforcement and two with internal shear stirrups) and one beam without stirrups and upgraded in shear with one layer of carbon/epoxy system. In all strengthened beams, fibers of the strengthening system were oriented in a 45° angle with the beam axis. Both control beams failed in shear, and the two counterparts without stirrups and with inorganic and organic matrix composites failed also in shear with the inorganic matrix composites of about 43% as effective as the resin-based FRP reinforcement in shear strength enhancement. However, for the other two strengthened beams failure changed from shear to failure in the compression zone.

Triantafillou and Papanicolaou [29] compared the performance of mortar and resin-based matrix for the textile reinforcement used in shear strengthening of RC beams. A total of 6 simply supported beams, deficient in shear, were tested under the action of two symmetric point loads. Four beams were tested under monotonic loading, whereas the remaining two beams were tested under quasi-static cyclic loading. Besides the conventional method of wrapping of the textile, spiral wrapping was also used. The test results revealed significant increase in shear strength of beams for the jackets prepared using closed-type textile reinforced mortar. For both types of jackets (conventional and spiral), 2 layers of TRM were enough for enhancing the shear strength of RC beams by more than the shear capacity of the unstrengthened beam.

Table 3
Comparison between TRM and FRP-strengthened beams tested at ambient temperature[a].

Researcher	Control Beam		TRM-strengthened beam					FRP-strengthened beam					TRM/FRP	
	Beam ID	$P_{u,co}$(kN)	Beam ID	No. of layers	$P_{u,TRM}$(kN)	$\Delta_{u,TRM}$(mm)	Failure mode	Beam ID	No. of layers	$P_{u,FRP}$(kN)	$\Delta_{u,FRP}$(mm)	Failure mode	Effectiveness ratio	Ultimate deflection ratio
Wu and Sun [107]	Plain	1.5	CFRC	1	3.2	2.4	FR	CFRP	1	6.9	2.4	D	0.31	0.97
Papanicolaou et al. [108]	C_fl	83.5	M4_fl	4	111.0	24	End-DB	R4_fl	4	125.0	22.2	FR	0.66	1.08
Toutanji and Deng [109]	PC	37	2IO-1	2	45.2	10.7	FR	2O-1	2	55.8	15.6	End-DB	0.44	0.69
	PC	37	3IO	3	55.6	14.50	FR	3O	3	55.8	15.85	End-DB	0.99	0.91
	PC	37	4IO-2	4	65.7	15.6	FR	4O-1	4	65.7	16.9	End-DB	1.00	0.92
Hashemi & Al-Mahaidi [110]	Control	121.2	MSF	2	132.1	31.7	D	ESF	2	161.7	32.2	D	0.27	0.98
Elsanadedy et al. [58]	BF-1	42.75	BF-3	5	59.5	34.15	FR	BF-5	1	64.1	22.05	FR	0.78	1.55
Raoof et al. [112]	CON	34.6	M1_C	1	39.0	13.2	S	R1_C	1	43.9	16	D	0.47	0.83
	CON	34.6	M3_C	3	55.3	14.7	D	R3_C	3	60.4	13.7	D	0.80	1.07
	CON	34.6	M7_BCo	7	46.9	18.4	FR	R7_BCo	7	54.2	24.9	FR	0.63	0.74
	CON	34.6	M7_G	7	43.2	10.3	FR	R7_G	7	48.2	18.4	FR	0.63	0.56
	CON	34.6	M3_C_EA	3	57.1	18.4	DS	R3_C_EA	3	83.7	26	FR	0.46	0.71
Average of whole data													0.62 ± 0.24	0.92 ± 0.26
Average of data with one and two layers of TRM													0.37 ± 0.10	0.87 ± 0.14
Average of data with 3 or more layers of TRM													**0.74 ± 0.19**	**0.94 ± 0.30**

[a] $P_{u,co}$ = ultimate load of control beam; $P_{u,TRM}$ = ultimate load of TRM-strengthened beam; $\Delta_{u,TRM}$ = ultimate deflection of TRM-strengthened beam; $P_{u,FRP}$ = ultimate load of FRP-strengthened beam; $\Delta_{u,FRP}$ = ultimate deflection of FRP-strengthened beam; End-DB = end debonding; FR = fiber rupture; D = TRM (or FRP) debonding from concrete substrate; S = slippage and partial rupture of the fibers through the mortar; DS = debonding of TRM from concrete substrate, followed by slippage of the fibers at the region where the longitudinal TRM meets the TRM U-jacket; SD = standard deviation; COV = coefficient pf variation.

Table 4
Comparison between TRM and FRP-strengthened beams tested at elevated temperature of 150 °C[a].

Researcher	TRM-strengthened beam					FRP-strengthened beam					TRM/FRP		Effectiveness ratio due to heating	
	Beam ID	n_f	$P_{u,TRM,T}$(kN)	$\Delta_{u,TRM,T}$(mm)	Failure mode	Beam ID	n_f	$P_{u,FRP,T}$(kN)	$\Delta_{u,FRP,T}$(mm)	Failure mode	Effectiveness ratio	Ultimate deflection ratio	TRM	FRP
Raoof & Bournas [113]	M1_C_150	1	37.7	9.1	S	R1_C_150	1	35.9	8.7	AF	2.38	1.05	0.70	0.14
	M3_C_150	3	44.7	8.9	D	R3_C_150	3	36.7	8.2	AF	4.81	1.09	0.49	0.08
	M7_BCo_150	7	41.1	13.7	S	R7_BCo_150	7	36.5	11.6	AF	3.42	1.18	0.53	0.10
	M7_G_150	7	38.8	10.3	S	R7_G_150	7	35.8	19.5	AF	3.50	0.53	0.49	0.09
	M3_C_EA_150	3	46.2	10.5	DS	R3_C_EA_150	3	57.5	25.0	AS	0.51	0.42	0.52	0.47
Average											**2.92 ± 1.60**	**0.85 ± 0.35**	**0.54 ± 0.09**	**0.17 ± 0.16**

[a] $P_{u,TRM,T}$ = ultimate load of TRM-strengthened beam at elevated temperature; $\Delta_{u,TRM,T}$ = ultimate deflection of TRM-strengthened beam at elevated temperature; $P_{u,FRP,T}$ = ultimate load of FRP-strengthened beam at elevated temperature; $\Delta_{u,FRP,T}$ = ultimate deflection of FRP-strengthened beam at elevated temperature; S = slippage and partial rupture of the fibers through the mortar; D = TRM debonding from concrete substrate including parts of concrete cover; DS = debonding of TRM from concrete substrate, followed by slippage of the fibers at the region where the longitudinal TRM meets the TRM U-jacket; AF = adhesive failure at the concrete-resin interface; AS = adhesive failure at the concrete-resin interface in the non-anchorage zone, followed by partial rupture and slippage of the fibers at the region where the longitudinal FRP meets the FRP U-jacket; SD = standard deviation; COV = coefficient pf variation.

Moreover, one layer of TRM was enough for enhancing the shear strength of RC beam by 72% of that of the control beam. However, a single layer of TRM was 55% as effective as the resin-based FRP. For the modeling purposes, authors suggested that the TRM jackets can be treated in the same way as the FRP jackets but with the adoption of experimental values of jacket effectiveness coefficients to be established through comprehensive experiments.

Blanksvärd et al. [71] compared the performance of TRM and FRP strengthening systems using carbon fabrics. Test results revealed that the TRM system increased the load capacity by up to 97%, relative to control unstrengthened specimen, and the failure mode was by rupture of the carbon fibers. The counterpart FRP system enhanced the load carrying capacity of the tested beams by 104% and failed by debonding.

Larbi et al. [115] examined the viability of using textile reinforced concrete plates for the retrofitting of concrete beams in shear. The performance of this system of strengthening was compared with a more prevalent system of CFRP strengthening. Three types of mortar-based systems were tried: (i) glass grid/mat with hydraulic mortar, (ii) glass mat with inorganic phosphate cement, and (iii) short metallic fibers with ultra-high performance mortar. The U-reinforcement and the side reinforcement were used for these systems. The performance of the textile reinforced mortar composites was found to be quantitatively at par with the CFRP. For predicting the shear capacity of TRM-strengthened RC beams, the Ritter-Morsch truss model was found to be appropriate. The test results of mortar-based composite indicated substantial enhancement in shear strength and flexural stiffness of beams. The U-shaped reinforcement was identified as the most effective method of shear strengthening.

Al-Salloum et al. [57] employed basalt-based TRM for upgrading the shear strength of concrete beams. Two types of mortar were used namely cementitious and polymer-modified cementitious. The number of textile layers were either two or four per side. The textile was attached to the beams such that the orientation of fibers was 0°/90° or 45°/-45°. Out of a total of ten beams, two were control, which were deficient in shear, and the remaining eight beams were strengthened for upgrading shear using TRM strengthening material. No internal shear reinforcement was provided in the shear spans of all the beams. The strengthening layers were bonded to the sides of shear spans. The test results revealed that the TRM composite was effective in enhancing the shear strength of RC beams by 36%–88%. The use of even 4 layers of textile per side could not prevent the brittle shear failure due to the use of weak basalt fibers. For beams having 4 layers of TRM each side, the 45°/-45° textile exhibited better performance than the 0°/90° textile. Further, in comparison to the cementitious mortar, the polymer-modified mortar was far better in improving the shear capacity. The tested RC beams were analyzed numerically using LS-DYNA software [111]. The parametric studies for TRM modeled, with and without mortar were also performed. FE model for half of one of the TRM-strengthened beams is shown in Fig. 25. The numerical study revealed that 12 layers of TRM would be approximately equivalent to a single layer of CFRP sheet and the TRM effectiveness ratio was about 97% of its FRP counterpart.

Tetta et al. [93] studied experimentally the performance of FRP and TRM strengthening system in enhancing the shear strength of concrete beams. Three wrapping schemes were tried such as full jacketing, U-wrapping, and side-bonding. Both strengthening systems employed same reinforcement but the two systems differed in the use of the binder. The textile used had same amount of carbon fibers in two orthogonal directions. Comparison of failure modes for some selected TRM-strengthened beams with their FRP counterparts is illustrated in Fig. 26. Although the FRP jacketing performed better than the TRM, the performance of TRM is dependent upon the number of textile layers and the strengthening configuration. The effectiveness factor of TRM with respect to FRP varies from 0.09 (for 1 layer of side-bonding) to 0.92 (for 2 layers of U-jacket). This highlights the effectiveness of TRM U-jacket as compared to the side-bonded jacket. However, for FRP jackets, the U-jacket was marginally more effective than the side-bonded jacket. For both FRP and TRM systems, full wrapping was found to be the most effective scheme. The increase in the number of layers from 1 to 2 resulted in the enhancement of FRP effectiveness by 1.35 and 1.2 times, respectively, for side-bonded and U-wrapped systems. On the other hand, the same increase for TRM jackets caused significant enhancement in its effectiveness by 7.8 and 2.6 times for side-bonded and U-wrapped systems, respectively. This substantial enhancement in the effectiveness of TRM jackets was due to the mechanical interlock formed by the overlapping textile layers, which changed the mode of failure from the local TRM failure (partial rupture of fibers with slipping of fibers from mortar) to the concrete substrate (jacket debonding and peeling off concrete cover).

Tzoura and Triantafillou [116] examined the performance of U-shaped TRM and FRP jackets in enhancing the shear capacity of RC T-beams under cyclic loadings of varying displacement amplitude. Other studied parameters included: fabrics of different kinds, number of layers, and anchorage. The anchorage system substantially enhanced the performance of FRP/TRM jackets. FRP jackets without anchorage were about twice as effective as the TRM. Nevertheless, the TRM jackets with anchorages was almost at par with the FRP jackets.

In another study, Tetta and Bournas [117] compared the performance of TRM jackets with FRP at elevated temperatures (100, 150, and 250 °C) in shear strengthening of RC T-beams. Studied parameters were: (i) retrofitting system (U-jacket, full wrapping, and side-bonding), (ii) number of layers (2 or 3), (iii) geometry and material of fabric, and (iv) anchorage system. At elevated temperature, the TRM was found to be substantially more effective in enhancing the shear strength of concrete beams as compared to the FRP. The increase in temperature from 100 to 150 °C reduced the effectiveness of FRP drastically. Whereas, the TRM was only slightly affected for the same increase in temperature and even up to 250 °C. At elevated temperature, the beams with side-bonded and U-jackets of FRP failed because of the failure of resin-concrete adhesion, as seen in Fig. 27(a), or slipping of fibers from the epoxy along with delamination of fabric employed for overlapping (for fully wrapped jackets), as depicted in Fig. 27(b). TRM-retrofitted beams exposed to elevated temperature failed also in shear due to either local damage in

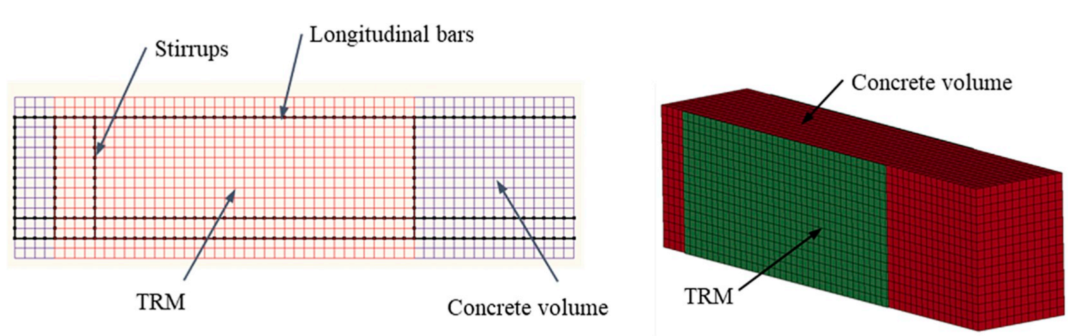

Fig. 25. FE mesh for one-half of the TRM-strengthened beams tested by Al-Salloum et al. [57].

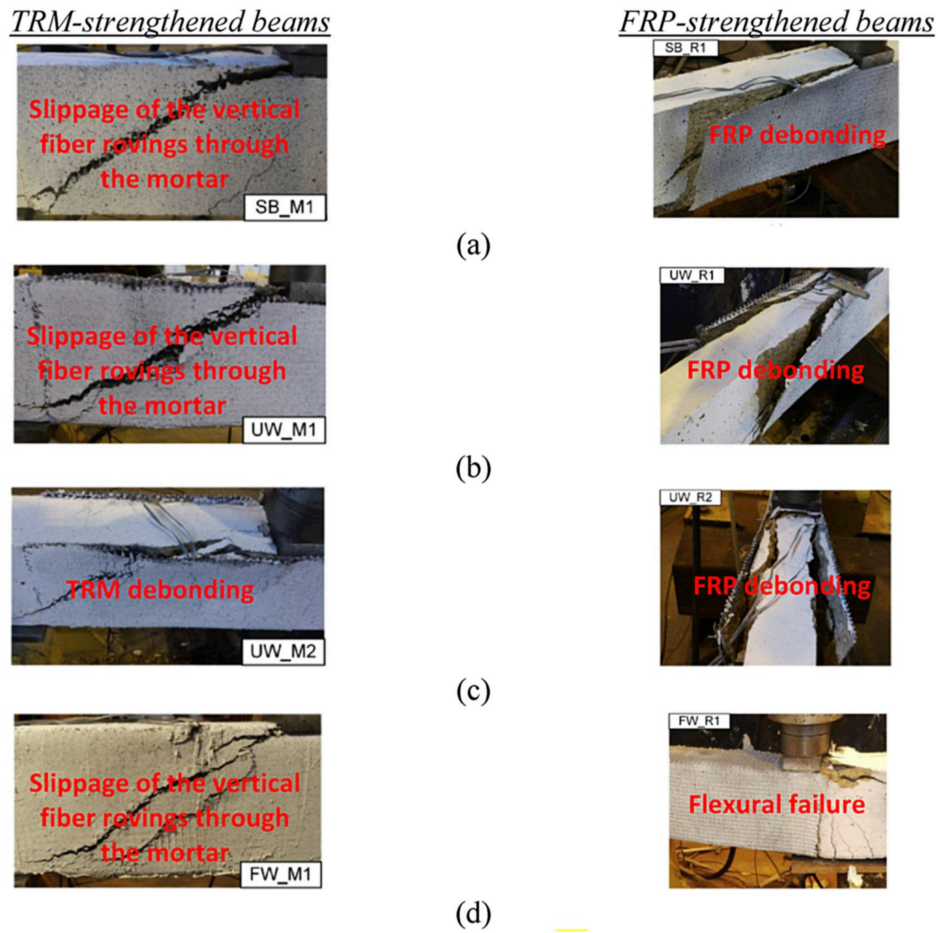

Fig. 26. Failure modes of beams tested by Tetta et al. [93]: (a) 1 layer of side-bonded jacket; (b) 1 layer of U-jacket; (c) 2 layers of U-jacket; (d) 1 layer of fully wrapped jacket.

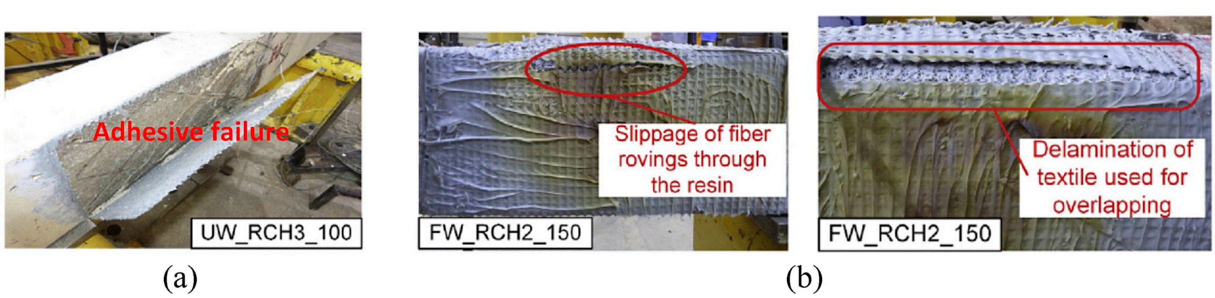

Fig. 27. Failure modes of FRP-strengthened beams tested by Tetta and Bournas [117]: (a) Three layers of U-wrapped jacket at 100 °C; (b) Two layers of fully wrapped jacket at 150 °C.

the jacket (slipping of fibers from mortar and partial fiber rupture (Fig. 28(a))) or debonding of the TRM jacket with peeling off concrete cover (Fig. 28(b)).

Gonzalez-Libreros et al. [118] investigated experimentally the performance of concrete beams retrofitted in shear using externally bonded FRP and TRM composites of carbon and steel. The effectiveness of anchorages and the effect of internal steel shear reinforcement ratio were also studied. For the steel FRP and TRM retrofitted RC beams having similar axial stiffness of strengthening material, the enhancement in shear capacity was almost same for beams having low volumetric ratio of stirrups with TRM versus FRP effectiveness ratios of 0.9. However, for beams with higher volumetric ratio of stirrups, TRM was considerably inferior to FRP composites with effectiveness ratio of 0.4. The beams having larger stirrup spacing exhibited greater increase in shear

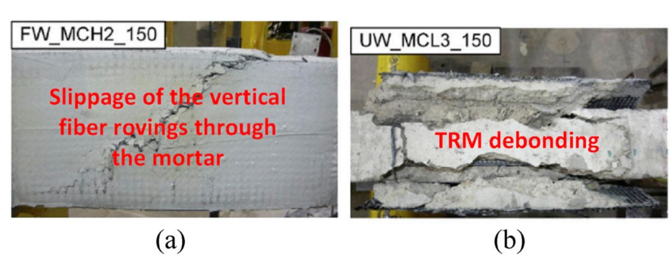

Fig. 28. Failure modes of TRM-strengthened beams tested by Tetta and Bournas [117]: (a) Two layers of fully wrapped jacket at 150 °C; (b) Three layers of U-wrapped jacket at 150 °C.

strength. All TRM-retrofitted RC beams without anchors displayed sudden failure in shear. The failure of carbon TRM-retrofitted RC beams was characterized by local debonding of composite and the slipping of fibers. On the other hand, the failure of steel TRM-retrofitted RC beams occurred by debonding of composite without any peeling off concrete cover. The interaction between internal and external shear reinforcement was more pronounced in FRP composites as compared to the TRM composites.

5.2. Discussion of main findings

5.2.1. Beams tested at ambient temperature

Summary of results for TRM-upgraded beams along with their FRP counterparts tested by previously discussed researchers at ambient temperature is illustrated in Table 5. From the table, it is concluded that for different strengthening configurations, full wrapping was the most effective in increasing the shear strength for both TRM and FRP systems, followed by U-wrapping whereas side-bonding was the least effective strengthening configuration. From the table, it is also evident that FRP-upgraded beams failed due to either flexural, or shear failure preceded by debonding of jacket from the concrete substrate with parts of concrete cover attached to the FRP laminates. However, failure of TRM-strengthened beams was due to either flexural, or shear failure preceded by either slippage of the vertical fiber rovings through the mortar and partial fibers rupture or debonding of the jacket with peeling off parts of the concrete cover. In order to compare the TRM and its FRP counterpart, TRM versus FRP effectiveness ratio was calculated for all counterparts shown in Table 5 from

$$\text{TRM versus FRP effectiveness ratio} = \frac{V_f\ (\text{TRM jacket})}{V_f\ (\text{FRP jacket})} \tag{4}$$

where V_f = shear strength contribution of TRM (or FRP) jacket = shear capacity of shear span of strengthened beam minus shear capacity of shear span of unstrengthened beam. It is evident from Table 5 that TRM is generally less effective in enhancing the shear strength of concrete beams than FRP jacketing, but the effectiveness depends on number of layers and the strengthening configuration. For the same textile material, increasing the number of TRM layers increased the effectiveness ratio of the TRM jacket and the least effectiveness was given by beams upgraded with one TRM layer per side with minimum and average effectiveness ratio of 0.09 and 0.49 as depicted in Table 5. However, the average TRM versus FRP effectiveness ratio for beams strengthened with two or more TRM layers per side was 0.85. It is therefore recommended to use at least two TRM layers per side for shear strengthening of RC beams, however, for FRP composites, one layer could be used. It is also noted from Table 5 that the use of anchors increased significantly the effectiveness of both TRM and FRP jackets.

5.2.2. Beams tested at high temperature

For the beams tested by Tetta and Bournas [117] at high temperature of 100 °C, 150 °C and 250 °C, TRM versus FRP effectiveness ratio were calculated using Eq. (4) and listed in Table 6. In addition, both TRM and FRP effectiveness ratios due to heating were assessed from

$$TRM\ (or\ FRP)\ effectiveness\ ratio\ due\ to\ heating = \frac{V_{f,T}}{V_{f,R}} \tag{5}$$

where $V_{f,T}$ = shear strength contribution of TRM (or FRP) jacket at elevated temperature and $V_{f,R}$ = shear strength contribution of TRM (or FRP) jacket at ambient temperature. These ratios are also enlisted in Table 6 for beams tested by Tetta and Bournas [117]. It is noted that TRM showed excellent behavior as retrofitting composite in enhancing the shear strength at elevated temperature; in fact, TRM displayed a mean effectiveness of 61% as compared to the ambient temperature. On the contrary FRP lost most of its effectiveness when exposed to elevated temperature, as seen in Table 6. It is also noted that among all strengthening configurations, full wrapping was the least to be affected by high temperature for both TRM and FRP jackets.

6. Design codes and guidelines

As far as design is concerned for external strengthening of RC structures using FRP or TRM composites, design codes, standards or guidelines have to be made ready and accessible to be used by practicing engineers. In searching of the literature, 10 guidelines/codes were found for the design of externally bonded FRP systems for strengthening RC structures (see Table 7). Out of the 10 guidelines/codes, three were

Table 5
Comparison between TRM and FRP-strengthened beams in shear and tested at ambient temperature[a].

Researcher	Strengthening configuration	TRM-strengthened beam				FRP-strengthened beam				TRM/FRP effectiveness ratio
		Beam ID	n_f (per side)	V_f (kN)	Failure mode	Beam ID	n_f (per side)	V_f (kN)	Failure mode	
Wiberg [114]	SB	T0A	1	96	SL-SH	T0E	1	222	DB-SH	0.43
Triantafillou & Papanicolaou [29]	FW	M1	1	42	SL-SH	R1	1	73	FL	0.57
	FW	M2	2	64	FL	R2	2	58	FL	1.09
Al-Salloum et al. [57]	SB	BS11	12	33	FL	BS12	1	34	FL	0.97
Tetta et al. [93]	SB	SB_M1	1	2.7	SL-SH	SB_R1	1	31	DB-SH	0.09
	UW	UW_M1	1	15	SL-SH	UW_R1	1	35	DB-SH	0.43
	FW	FW_M1	1	34	SL-SH	FW_R1	1	56	FL	0.60
	SB	SB_M2	2	21	DB-SH	SB_R2	2	42	DB-SH	0.51
	UW	UW_M2	2	39	DB-SH	UW_R2	2	43	DB-SH	0.92
Tzoura and Triantafillou [116]	UW	L2	2	13	DB-SH	RL2	2	26	DB-SH	0.52
	UW-A	L2A15	2	57	DB-SH	RL2A15	2	65	DB-SH	0.88
Tetta and Bournas [117]	UW	UW_MCH3	3	45	DB-SH	UW_RCH3	3	50	DB-SH	0.90
	FW	FW_MCH2	2	58	FL	FW_RCH2	2	57	FL	1.02
Gonzalez-Libreros et al. [118]	UW	S1-FRCM-F4-UN	1	35	DB-SH	S1-FRP-F2-UN	1	38	DB-SH	0.90
	UW	S2-FRCM-F4-UN	1	18	DB-SH	S2-FRP-F2-UN	1	44	FL	0.40
Average of whole data										0.68 ± 0.29
Average of data with one layer of TRM per side										0.49 ± 0.25
Average of data with 2 or more layers of TRM per side										**0.85 ± 0.22**

[a] n_f = No. of TRM (or FRP) layers per side; V_f = shear strength contributed by TRM (or FRP) jacket; SB = side-bonded jacket; UW = U-wrapped jacket; UW-A= U-wrapped jacket with anchorage; FW = fully wrapped jacket; SL-SH = shear failure preceded by slippage of the vertical fiber rovings through the mortar and partial fibers rupture; DB-SH = shear failure preceded by debonding of the jacket with peeling off parts of the concrete cover; FL = flexural failure.

Table 6
Comparison between TRM and FRP-strengthened beams in shear and tested at elevated temperature[a].

Researcher	Strengthening configuration	TRM-strengthened beam					FRP-strengthened beam					TRM/FRP effectiveness ratio	Effectiveness due to heating	
		Beam ID	n_f (per side)	$V_{f,R}$ (kN)	At elevated temperature		Beam ID	n_f (per side)	$V_{f,R}$ (kN)	At elevated temperature				
					$V_{f,T}$ (kN)	Failure mode				$V_{f,T}$ (kN)	Failure mode		TRM	FRP
Tetta and Bournas [117]	Beams tested at temperature of 100 °C													
	UW	UW_MCH3_100	3	45	31	DB-SH	UW_RCH3_100	3	50	20	AF-SH	1.55	0.69	0.40
	Beams tested at temperature of 150 °C													
	SB	SB_MCH2_150	2	21	11	SL-SH	SB_RCH2_150	2	42	0	AF-SH	∞	0.52	0.00
	SB	SB_MCH3_150	3	33	17	DB-SH	SB_RCH3_150	3	NA	0	AF-SH	∞	0.52	–
	UW	UW_MCH2_150	2	39	20	SL-SH	UW_RCH2_150	2	43	6	AF-SH	3.33	0.51	0.14
	UW	UW_MCH3_150	3	45	25	DB-SH	UW_RCH3_150	3	50	6	AF-SH	4.17	0.56	0.12
	FW	FW_MCH2_150	2	58	48	SL-SH	FW_RCH2_150	2	57	44	SL/DL-SH	1.09	0.83	0.77
	Beams tested at temperature of 250 °C													
	UW	UW_MCH3_250	3	45	29	DB-SH	UW_RCH3_250	NA	NA	NA	NA	–	0.64	–
Average													**0.61 ± 0.12**	**0.29 ± 0.29**

[a] n_f = No. of TRM (or FRP) layers per side; $V_{f,R}$ = shear strength contributed by TRM (or FRP) jacket at ambient temperature; $V_{f,T}$ = shear strength contributed by TRM (or FRP) jacket at elevated temperature; SB = side-bonded jacket; UW = U-wrapped jacket; FW = fully wrapped jacket; DB-SH = shear failure preceded by debonding of the jacket with peeling off parts of the concrete cover; AF-SH = shear failure preceded by adhesive failure at the resin-concrete interface; SL-SH = shear failure preceded by slippage of the vertical fiber rovings through the mortar and partial fibers rupture; SL/DL-SH = shear failure preceded by slippage of the vertical fiber rovings through the epoxy resin and delamination of the textile used for overlapping; NA = not available data.

Table 7
Available design guidelines (or code provisions) on externally bonded FRP (or TRM) systems for strengthening RC structures.

FRP systems		TRM systems	
Guideline/Code	Country	Guideline/Code	Country
ACI 440.2R-17 [49]	USA	ACI 549.4R-13 [31]	USA
NCHRP Rpt 655-10 [119]	USA		
ISIS Design Manual No. 4–2008 [120]	Canada		
EN 1998-3 [121]	Europe		
fib Bulletin 14–2001 [27]	Europe		
CS TR55-2012 [122]	UK		
CNR-DT 200 R1/2013 [123]	Italy		
JSCE-01 [124]	Japan		
CECS 146:2003 [125]	China		
ECP 208–2005 [126]	Egypt		

developed in North America – two in the United States [49,119] and one in Canada [120]. Another four guidelines/codes for FRP-strengthened RC members were developed in Europe – one by the European Committee for Standardization [121], one by the European *fib* Task Group 9.3 [27], one in the UK [122], and one in Italy [123]. Another two design guidelines were developed in Asia [124,125], and the last one was developed in Africa by the Egyptian Code Committee [126]. However, as seen in Table 7, the American ACI 549.4R-13 [31] is currently the only available guideline for design and construction of externally bonded TRM systems despite their widespread application.

7. Conclusions and recommendations

The main conclusions drawn from this review paper can be summarized as follows:

1. At ambient temperature, TRM is generally inferior to FRP in enhancing the flexural and shear capacity of RC beams. TRM effectiveness depends on number of layers, strengthening configuration, coating of textile material and type of mortar selected. TRM effectiveness increased as the number of layers is increased. Coating the dry textile fibers with epoxy adhesive significantly enhanced the performance of TRM material. Using polymer modified cementitious mortars gave better results than conventional cementitious mortar.
2. At high temperature exposure, TRM exhibited excellent performance as strengthening material compared to its effectiveness at ambient temperature. At 150 °C TRM maintained an average effectiveness of 54% and 59% for flexural and shear strengthening applications, respectively, compared to its effectiveness at ambient temperature, contrary to FRP which lost most of its effectiveness when subjected to high temperature of 150 °C.
3. In the design of TRM composites as strengthening schemes, it is recommended to ignore the contribution of mortar and use the properties of the bare textile alone. It is also recommended to use at least three TRM layers for flexural strengthening of RC beams and two layers per side for shear strengthening of RC beams. It is worth mentioning that these recommendations are based on very limited experimental data available in literature, and less number of TRM layers can be recommended once more test data become available.

Based on review of available literature on effectiveness of TRM compared with FRP composites in strengthening of concrete structures, gaps exist in current knowledge and further research is needed. It is therefore recommended to:

1. Conduct an extensive experimental study to investigate the bond behavior at TRM-concrete interface by varying different parameters such as number of TRM layers, type of mortar, type of textile fabric and strength of the substrate concrete. The obtained data along with

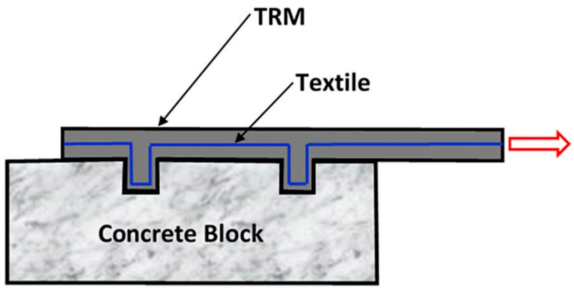

Fig. 29. Concept of TRM anchorage system with grooves in concrete.

database collected from literature shall be used to establish bond-slip relationships for TRM-to-concrete interface.

2. Study experimentally the bond behavior at TRM-concrete interface in the following cases: (i) after applying a bonding primer at the concrete surface, (ii) during exposure to standard fire test as per ASTM E119 [127], and (iii) when anchoring the TRM using grooves created in the concrete substrate as shown in Fig. 29.
3. Study experimentally the behavior of TRM-strengthened RC beams during exposure to standard fire test as per ASTM E119 [127].
4. Study experimentally the effectiveness of TRM compared with externally bonded FRP composites in: enhancing the flexural capacity of RC slabs, increasing the shear capacity of RC deep beams, and upgrading the torsional capacity of RC beams.
5. Study numerically the behavior of TRM-strengthened beams in flexure and shear by creating a FE model that accounts for different failure modes such as interlaminar debonding, fabric slippage inside the matrix, debonding at TRM-concrete substrate, peeling off parts of concrete cover and textile rupture. This model should be validated with experimental database from literature. The validated model should be then used to assess the effect of different parameters of interest such as number of TRM layers, type of mortar, and end anchorage.

Acknowledgement

The authors are grateful to the Deanship of Scientific Research, King Saud University, for funding through Vice Deanship of Scientific Research Chairs.

Appendix A. Supplementary data

Supplementary data to this article can be found online at https://doi.org/10.1016/j.compositesb.2019.106947.

References

[1] ACI 546.1R. Guide to concrete repairvol. 546. Farmington Hills, MI: Amserican Concrete Institute (ACI) Committee; 2014.
[2] Escrig C, Gil L, Bernat-Maso E, Puigvert F. Experimental and analytical study of reinforced concrete beams shear strengthened with different types of textile-reinforced mortar. Constr Build Mater 2015;83:248–60.
[3] Sezen H. Effectiveness of repair and strengthening methods for reinforced concrete columns and beam-column joints. In: Structures congress, vol. 10; 2012. p. 2015–24. Chicago, IL.
[4] Tan KH. Beam strengthening by external post-tensioning: design recommendations. IES J Part A Civ Struct Eng 2016;7(4):219–28.
[5] Alsayed SH, Al-Salloum YA, Almusallam TH, Siddiqui NA. Seismic response of FRP-upgraded exterior RC beam-column joints. ASCE J Compos Constr 2010;14 (2):195–208.
[6] Alsayed SH, Almusallam TH, Al-Salloum YA, Siddiqui NA. Seismic rehabilitation of corner RC beam-column joints using CFRP composites. ASCE J Compos Constr 2010;14(6):681–92.
[7] Al-Salloum YA, Almusallam TH, Alsayed SH, Siddiqui NA. Seismic behavior of as-built, ACI-complying, and CFRP-repaired exterior RC beam-column joints. ASCE J Compos Constr 2010;15(4):522–34.
[8] Alhaddad MS, Siddiqui NA, Abadel AA, Alsayed SH, Al-Salloum YA. Numerical investigations on the seismic behavior of FRP and TRM upgraded RC exterior beam-column joints. ASCE J Compos Constr 2011;16(3):308–21.
[9] Elsanadedy HM, Abbas H, Al-Salloum YA, Almusallam TH. Prediction of intermediate crack debonding strain of externally bonded FRP laminates in RC beams and one-way slabs. ASCE J Compos Constr 2014;18(5):04014008.
[10] Mosallam A, Elsanadedy HM, Almusallam TH, Al-Salloum YA, Alsayed SH. Structural evaluation of reinforced concrete beams strengthened with innovative bolted/bonded advanced FRP composites sandwich panels. Compos Struct 2015; 124:421–40.
[11] Almusallam T, Al-Salloum Y, Alsayed S, Iqbal R, Abbas H. Effect of CFRP strengthening on the response of RC slabs to hard projectile impact. Nucl Eng Des 2015;286:211–26.
[12] Elsanadedy HM, Abbas H, Al-Salloum YA, Almusallam TH. Closure to â€œPrediction of intermediate crack debonding strain of externally bonded FRP laminates in RC beams and one-way Slabsâ€ by HM Elsanadedy, H. Abbas, YA Al-salloum, and TH almusallam. *ASCE*. J Compos Constr 2014;19(2):07014004.
[13] Abbas H, Abadel AA, Almusallam T, Al-Salloum Y. Effect of CFRP and TRM strengthening of RC slabs on punching shear strength. Lat Am J Solid Struct 2015; 12(9):1616–40.
[14] Elsanadedy HM, Al-Salloum YA, Al-Zaheri ZM, Alsayed SH, Abbas H. Behavior and design aspects of FRP-strengthened URM walls under out-of-plane loading. ASCE J Compos Constr 2016;20(6):04016048.
[15] Alsayed SH, Elsanadedy HM, Al-Zaheri ZM, Al-Salloum YA, Abbas H. Blast response of GFRP-strengthened infill masonry walls. Constr Build Mater 2016; 115:438–51.
[16] Abadel A, Abbas H, Almusallam T, Al-Salloum Y, Siddiqui N. Local impact damage response of CFRP strengthened concrete slabs. Procedia Engineer 2017; 173:85–92.
[17] Almusallam T, Al-Salloum Y, Elsanadedy H, Alshenawy A, Iqbal R. Behavior of FRP-strengthened RC beams with large rectangular web openings in flexure zones: experimental and numerical study. Int J Concr Struct M 2018;12(1):47.
[18] Elsanadedy HM, Al-Salloum YA, Almusallam TH, Alshenawy AO, Abbas H. Experimental and numerical study on FRP-upgraded RC beams with large rectangular web openings in shear zones. Constr Build Mater 2019;194:322–43.
[19] https://www.structural.net/case-studies/strengthening-restoration-of-casino/.
[20] Jãlio ENBS, Branco FAB. Reinforced concrete jacketing - interface influence on cyclic loading response. ACI Struct J 2008;105(4):471–7.
[21] https://www.schwagerdavis.com/divisions/structural-retrofit/.
[22] https://www.horseen.com/project/Bonded-steel-plate-reinforcement-Zhengzhou-department-store.
[23] Aykac S, Kalkan I, Asce AM, Aykac B, Karahan S, Kayar S. Strengthening and repair of reinforced concrete beams using external steel plates. J Struct Eng 2013; 139:929–39.
[24] De Lorenzis L, Nanni A, La Tegola A. Strengthening of reinforced concrete structures with near surface mounted FRP rods. In: Int. Meeting on composite materials, PLAST 2000, milan, Italy, may 9-11; 2000.
[25] Bournas D, Triantafillou T. Strengthening of reinforced concrete columns with near-surface-mounted FRP or stainless steel. ACI Struct J 2009;106(4):495–505.
[26] https://www.quakewrap.com/beams.php.
[27] Fib bulletin 14. Externally bonded FRP reinforcement for RC structures. Technical Report prepared by the Working Party EBR of Task Group 9.3. Lausanne, Switzerland: International Federation for Structural Concrete; 2001.
[28] Papanicolaou CG, Triantafillou TC, Papathanasiou M, Karlos K. Textile reinforced mortar (TRM) versus FRP as strengthening material of URM walls: out-of-plane cyclic loading. Mater Struct 2008;41(1):143–57.
[29] Triantafillou TC, Papanicolaou CG. Shear strengthening of reinforced concrete members with textile reinforced mortar (TRM) jackets. Mater Struct 2006;39. 93â€"03.
[30] Triantafillou TC, Papanicolaou CG, Zissimopoulos P, Laourdekis T. Concrete confinement with textile reinforced mortar (TRM) jackets. ACI Struct J 2006;103 (1):28–37.
[31] ACI Committee 549. Guide to design and construction of externally bonded fabric-reinforced cementitious matrix (FRCM) systems for repair and strengthening concrete and masonry structures (ACI 549.4R-13). Farmington Hills, MI: American Concrete Institute; 2013.
[32] Gudonis E, Timinskas E, Gribniak V, Kaklauskas G, Arnautov AK, TamulÄ—nas V. FRP reinforcement for concrete structures: state-of-the-art review of application and design. Engineering Structures and Technologies, Taylor & Francis 2013;5 (4):147–58.
[33] Mukhtar FM, Faysal RM. A review of test methods for studying the FRP-concrete interfacial bond behavior. Constr Build Mater 2018;169:877–87.
[34] Amran YHM, Alyousef R, Rashid RSM, Alabduljabbar H, Hung C. Properties and applications of FRP in strengthening RC structures: a review. Structure (Lond) 2018;16:208–38.
[35] Hollaway LC. A review of the present and future utilisation of FRP composites in the civil infrastructure with reference to their important in-service properties. *Constr Build Mater* 2010;24:2419–45.
[36] Firmo JP, Correia JR, Bisby LA. Fire behaviour of FRP-strengthened reinforced concrete structural elements: a state-of-the-art review. Comp Part B 2015;80: 198–216.
[37] Awani O, El-Maaddawy T, Ismail N. Fabric-reinforced cementitious matrix: a promising strengthening technique for concrete structures. Constr Build Mater 2017;132:94–111.
[38] Koutas LN, Tetta Z, Bournas DA, Triantafillou TC. Strengthening of concrete structures with textile reinforced mortars: state-of-the-art review. J Compos Constr 2019;23(1):03118001.

[39] ACI 440R. Report on fiber-reinforced polymer (FRP) reinforcement for concrete structuresvol. 440. Farmington Hills, MI: American Concrete Institute (ACI) Committee; 2007.
[40] GangaRao HVS, Vijay PV. Feasibility review of FRP materials for structural applications. Vicksburg, MS: *Engineering Research & Development Center - US Army Corps of Engineers*; 2010.
[41] Silfwerbrand JL. Failure, distress and repair of concrete structures. In: Delatte N, editor. Failure, distress and repair of concrete structures. Boca Rotan, FL: CRC Press; 2009.
[42] Aljazaeri ZR, Myers JJ. Fatigue and flexural behavior of reinforced concrete beams strengthened with a fiber reinforced cementitious matrix. ASCE J Compos Constr 2017;21(1):04016075.
[43] Babaeidarabad S, Loreto G, Nanni A. Flexural strengthening of RC beams with an externally bonded fabric-reinforced cementitious matrix. ASCE J Compos Constr 2014;18(5):1–12.
[44] Dâ€™Ambrisi A, Focacci F. Flexural strengthening of RC beams with cement-based composites. ASCE J Compos Constr 2011;15(5):707–20.
[45] Gil L, Escrig C, Bernat E. Bending performance of concrete beams strengthened with textile reinforced mortar TRM. Key Eng Mater 2014;601:203–6.
[46] Ombres L. Flexural analysis of reinforced concrete beams strengthened with a cement based high strength composite material. Compos Struct 2011;94(1): 143–55.
[47] Si Larbi A, Agbossou A, Hamelin P. Experimental and numerical investigations about textile-reinforced concrete and hybrid solutions for repairing and/or strengthening reinforced concrete beams. Compos Struct 2013;99:152–62.
[48] ASTM. Standard test method for tensile properties of polymer matrix composite materials. West Conshohocken, PA: American Society for Testing and Materials; 2008. ASTM D3039/D3039M â€“ 08.
[49] ACI Committee 440. Guide for the design and construction of externally bonded FRP systems for strengthening concrete structures. Farmington Hills, MI: American Concrete Institute; 2017. ACI 440.2R-17.
[50] Elsanadedy HM. Seismic performance and analysis of ductile composite-jacketed reinforced concrete bridge columns. Irvine: University of California; 2002. Ph.D. Thesis.
[51] https://www.luckett-farley.com/Blog/Article/119/FRP-Concrete-Strengthening-101.
[52] Ma R. Seismic retrofit and repair of reinforced concrete columns using advanced composite materials. University of Southern California; August 1999. Ph.D. Thesis.
[53] Bournas DA, Triantafillou TC, Zygouris K, Stavropoulos F. Textile-reinforced mortar versus FRP jacketing in seismic retrofitting of RC columns with continuous or lap-spliced deformed bars. ASCE J Compos Constr 2009;13:360–71.
[54] Colajanni P, Fossetti M, MacAluso G. Effects of confinement level, cross-section shape and corner radius on the cyclic behavior of CFRCM confined concrete columns. Constr Build Mater 2014;55:379–89.
[55] Papanicolaou CG, Triantafillou TC, Papathanasiou M, Karlos K. Textile reinforced mortar (TRM) versus FRP as strengthening material of URM walls: in-plane cyclic loading. Mater Struct 2007;40(10):1081–97.
[56] Al-Salloum YA, Siddiqui NA, Elsanadedy HM, Abadel AA, Aqel MA. Textile-reinforced mortar versus FRP as strengthening material for seismically deficient RC beam-column joints. ASCE J Compos Constr 2011;15(6):920–33.
[57] Al-Salloum YA, Elsanadedy HM, Alsayed SH, Iqbal RA. Experimental and numerical study for the shear strengthening of reinforced concrete beams using textile-reinforced mortar. ASCE J Compos Constr 2012;16(1):74–90.
[58] Elsanadedy HM, Almusallam TH, Alsayed SH, Al-Salloum YA. Flexural strengthening of RC beams using textile reinforced mortar - experimental and numerical study. Compos Struct 2013;97:40–55.
[59] Triantafillou TC, Papanicolaou CG. Textile reinforced mortars (TRM) versus fibre reinforced polymers (FRP) as strengthening materials of concrete structures. In: Seventh int. Symp. Of the fiber-reinforced polymer reinforcement for reinforced concrete structures. FRPRCS; 2005. p. 99–118.
[60] Nanni A. Guide to design and construction of externally bonded fabric-reinforced cementitous matrix (FRCM) systems for repair and strengthening concrete structures. ACI Webinar Notes 2014;1â€"18.
[61] ICC Evaluation Service AC434. Acceptance criteria for masonry and concrete strengthening using fiber-reinforced cementitious matrix (FRCM) composite systems. J Chem Inf Model 2013;53. Birmingham, AL.
[62] Loreto G, Leardini L, Arboleda D, Nanni A. Performance of RC slab-type elements strengthened with fabric-reinforced cementitious-matrix composites. ASCE J Compos Constr 2013;18(3):1–9. A4013003.
[63] Yao Y, Zhu D, Zhang H, Li G, Mobasher B, Asce M. Tensile behaviors of basalt, carbon, glass, and aramid fabrics under various strain rates. J Mater Civ Eng 2016;28(9):1–10.
[64] Michels J, Zwicky D, Scherer J, Harmanci YE, Motavalli M. Structural strengthening of concrete with fiber reinforced cementitious matrix (FRCM) at ambient and elevated temperature â€“ Recent investigations in Switzerland. Adv Struct Eng 2014;17(12):1785–800.
[65] Ruredil. Instructions for the planning of static consolidation interventions through the use of fibre reinforced cementitious matrix -FRCM. Di. Te. R - ruredilâ€™s Technical Department. 2008. Retrieved from, http://english.ruredil.it/Planning.pdf. on August 20, 2014.
[66] Arboleda D, Carozzi FG, Nanni A, Poggi C. Testing procedures for the uniaxial tensile characterization of fabric-reinforced cementitious matrix composites. ASCE J Compos Constr 2016;20(3). 04015063.
[67] ASTM. Standard test method for compressive strength of hydraulic cement mortars (using 2-in. or [50-mm] cube specimens). West Conshohocken, *PA*: ASTM C109/C109M, American Society for Testing and Materials; 2008.
[68] ASTM. Method of test for tensile strength of hydraulic cement mortars. West Conshohocken, *PA*: ASTM C190, American Society for Testing and Materials; 1985.
[69] Alsayed SH, Al-Salloum YA, Almusallam TH, Khan MI. Classification and testing performance of concrete repair materials for durable repair under local environmental conditions. In: Final report, applied national research program, research No. DSR-AR-2-42. Saudi Arabia: King Saud University; 2008.
[70] De Santis S, Carozzi FG, de Felice G, Poggi C. Test methods for textile reinforced mortar systems. Compos B Eng 2017;127:121–32.
[71] BlanksvÃ¤rd T, TÃ¤ljsten B, Carolin A. Shear strengthening of concrete structures with the use of mineral based composites. ASCE J Compos Constr 2009;13(1): 25–34.
[72] Lu XZ, Teng JG, Ye LP, Jiang JJ. Bond-slip models for sheets/plates bonded to concrete. Eng Struct 2005;27(6):920–37.
[73] Mohammadi T, Wan B, Harries KA. Bondâ€"slip behavior of fiber-reinforced polymer/concrete interface in single shear pull-out and beam tests. J Reinf Plast Compos 2016;35(5):375–86.
[74] Ko H, Matthys S, Palmieri A, Sato Y. Development of a simplified bond stressâ€"slip model for bonded FRPâ€"concrete interfaces. Constr Build Mater 2014;68:142–57.
[75] Sayed-Ahmed EY, Bakay R, Shrive NG. Bond strength of FRP laminates to concrete: state-of-the-Art Review. Electron J Struct Eng 2009;9:45–61.
[76] Almusallam TH, Elsanadedy HM, Al-Salloum YA. Effect of longitudinal steel ratio on behavior of RC beams strengthened with FRP composites â€“ Experimental and FE study. ASCE J Compos Constr 2015;19(1).
[77] Elsanadedy HM, Almusallam TH, Alsayed SH, Al-Salloum YA. Experimental and FE study on RC one-way slabs upgraded with FRP composites. KSCE J Civ Eng 2015;19(4):1024–40.
[78] Brosens K, Van Gemert D. Anchorage design for externally bonded carbon fiber-reinforced polymer laminates. In: Proceedings of the FRPRCS-4, SP-188. ACI; 1999. p. 635–45.
[79] Neubauer U, Rostasy FS. Bond failure of concrete fiber reinforced polymer plates at inclined cracks-experiments and fracture mechanics model. In: Proc of 4th international symposium on fiber reinforced polymer reinforcement for reinforced concrete structures, SP-188. Farmington Hills (MI): ACI; 1999. p. 369–82.
[80] Monti M, Renzelli M, Luciani P. FRP adhesion in uncracked and cracked concrete zones. In: Proc of 6th international symposium on FRP reinforcement for concrete structures. Singapore: World Scientific Publications; 2003. p. 183–92.
[81] Nakaba K, Kanakubo T, Furuta T, Yoshizawa H. Bond behavior between fiber-reinforced polymer laminates and concrete. ACI Struct J 2001:359–67.
[82] Savioa M, Farracuti B, Mazzotti D. Non-linear bondâ€"slip law for FRP concrete interface. In: Proc of 6th international symposium on FRP reinforcement for concrete structures. Singapore: World Scientific Publications; 2003. p. 163–72.
[83] Dai JG, Ueda T. Local bond stress slip relations for FRP sheets concrete interfaces. In: Proc of 6th international symposium on FRP reinforcement for concrete structures. Singapore: World Scientific Publications; 2003. p. 143–52.
[84] Dai JG, Ueda T, Sato Y. Development of the nonlinear bond stressâ€"slip model of fiber reinforced plastics sheet-concrete interfaces with a simple method. J Compos Constr 2005;9(1):52–62.
[85] Awani O, El Refai A, El-Maaddawy T. Bond characteristics of carbon fabric reinforced cementitious matrix in double shear tests. Constr Build Mater 2015; 101:39–49.
[86] Dâ€™Ambrisi A, Feo L, Focacci F. Bond-slip relations for PBO-FRCM materials externally bonded to concrete. Compos B Eng 2012;43(8):2938–49.
[87] Ombres L. Analysis of the bond between fabric reinforced cementitious mortar (FRCM) strengthening systems and concrete. Compos B Eng 2015;69:418–26.
[88] Dâ€™Antino T, Sneed LH, Carloni C, Pellegrino C. Effect of the inherent eccentricity in single-lap direct-shear tests of PBO FRCM-concrete joints. Compos Struct 2016;142:117–29.
[89] Hashemi S, Al-Mahaidi R. Investigation of bond strength and flexural behaviour of FRP-strengthened reinforced concrete beams using cement based adhesives. Aust J Struct Eng 2010;11(2):129–39.
[90] Sneed LH, Dâ€™Antino T, Carloni C. Investigation of bond behavior of polyparaphenylene benzobisoxazole fiber-reinforced cementitious matrix composite-concrete interface. ACI Mater J 2014;111(5):569–80.
[91] Dâ€™Ambrisi A, Feo L, Focacci F. Experimental analysis on bond between PBO-FRCM strengthening materials and concrete. Compos B Eng 2013;44(1):524–32.
[92] Raoof SM, Koutas LN, Bournas DA. Bond between textile-reinforced mortar (TRM) and concrete substrates: experimental investigation. Compos B Eng 2016; 98:350–61.
[93] Tetta ZC, Koutas LN, Bournas DA. Textile-reinforced mortar (TRM) versus fiber-reinforced polymers (FRP) in shear strengthening of concrete beams. Compos B Eng 2015;77:338–48.
[94] Raoof SM. Flexural strengthening of reinforced concrete beams with textile reinforced mortar (TRM). Department of Civil Engineering, The University of Nottingham; 2015. PhD annual report (2nd year).
[95] Yao J, Teng J, Chen J. Experimental study on FRP-to-concrete bonded joints. Compos B Eng 2005;36(2):99–113.
[96] Ascionea L, Carozzi FG, Dâ€™Antino T, Poggi C. New Italian guidelines for design of externally bonded Fabric-Reinforced Cementitious Matrix (FRCM) systems for repair and strengthening of masonry and concrete structures. Procedia Structural Integrity 2018;11:202–9.

[97] Jung K, Hong K, Han S, Park J, Kim J. Prediction of flexural capacity of RC beams strengthened in flexure with FRP fabric and cementitious matrix. Int J Polym Sci 2015:11. 2015, Article ID 868541.
[98] Blontrock H. Analysis and modeling of the fire resistance of concrete elements with externally bonded FRP reinforcement. PhD Thesis. Belgium: Ghent University; 2003.
[99] Firmo JP, Pitta D, Correia JR, Tiago C, Arruda MRT. Experimental characterization of the bond between externally bonded reinforcement (EBR) CFRP strips and concrete at elevated temperatures. Cement Concr Compos 2015; 60:44–54.
[100] Gamage JCPH, Wong MB, Al-Mahadi R. Performance of CFRP strengthened concrete members under elevated temperatures. In: Proc. Of the int. Symp. On bond behaviour of FRP in structures (BBFS 2005); 2005. Hong Kong, China.
[101] Klamer EL. Influence of temperature on concrete beams strengthened in flexure with CFRP. Ph.D. Thesis. Eindhoven, Netherlands: Eindhoven University of Technology; 2009.
[102] Klamer EL, Hordijk DA, Janssen HJM. The influence of temperature on the debonding of externally bonded CFRP. In: Proc. Of 7th int. Symp. On fiber-reinforced (FRP) polymer reinforcement for concrete structures; 2005. p. 1551–70. New Orleans, USA.
[103] Leone M, Matthys S, Aiello MA. Effect of elevated service temperature on bond between FRP EBR systems and concrete. Compos B Eng 2009;40(1):85–93.
[104] Wu ZS, Iwashita K, Yagashiro S, Ishikawa T, Hamaguchi Y. Temperature effect on bonding and debonding behavior between FRP sheets and concrete. J Soc Mater Sci Jpn 2005;54(5):474–80.
[105] Raoof SM, Bournas DA. Bond between TRM versus FRP composites and concrete at high temperatures. Compos B Eng 2017;127:150–65.
[106] Kurtz S, Balaguru P. Comparison of inorganic and organic matrices for strengthening of RC beams with carbon sheets. J Struct Eng-ASCE 2001;127(1): 35–42.
[107] Wu HC, Sun P. Fiber reinforced cement based composite sheets for structural retrofit. In: Chen, Teng, editors. proc. Of the int. Symp. On bond behaviour of FRP in structures (BBFS 2005); 2005. p. 343–8.
[108] Papanicolaou CG, Triantafillou TC, Bournas DA, Lontou PV. TRM as strengthening and seismic retrofitting material of concrete structures. In: Proc. Of 1st int. Conf. On textile reinforced concrete (ICTRC). Germany: RWTH Aachen University; 2006. p. 331–40.
[109] Toutanji H, Deng Y. Comparison between organic and inorganic matrices for RC beams strengthened with carbon fiber sheets. ASCE J Compos Constr 2007;11(5): 507–13.
[110] Hashemi S, Al-Mahaidi R. Experimental and finite element analysis of flexural behavior of FRP-strengthened RC beams using cement-based adhesives. Constr Build Mater 2012;26:268–73.
[111] Livermore Software Technology Corporation (LSTC). LS-DYNA userâ€™s keyword manual (nonlinear dynamic analysis of structures in three dimensions), vol. 1. Livermore, California: LSTC; 2007. Version 971.
[112] Raoof SM, Koutas LN, Bournas DA. Textile-reinforced mortar (TRM) versus fibre-reinforced polymers (FRP) in flexural strengthening of RC beams. Constr Build Mater 2017;151:279–91.
[113] Raoof SM, Bournas DA. TRM versus FRP in flexural strengthening of RC beams: behaviour at high Temperatures. Constr Build Mater 2017;154:424–37.
[114] Wiberg A. Strengthening of concrete beams using cementitious carbon fibre composites. Doctoral Thesis. Stockholm: Royal Institute of Technology; 2003.
[115] Larbi AS, Contamine R, Ferrier E, Hamelin P. Shear strengthening of RC beams with textile reinforced concrete (TRC) plate. Constr Build Mater 2010;24: 1928–36.
[116] Tzoura E, Triantafillou TC. Shear strengthening of reinforced concrete T-beams under cyclic loading with TRM or FRP jackets. Mater Struct 2016;49:17–28.
[117] Tetta ZC, Bournas DA. TRM vs FRP jacketing in shear strengthening of concrete members subjected to high temperatures. Compos B Eng 2016;106:190–205.
[118] Gonzalez-Libreros JH, Sneed LH, Dâ€™Antino T, Pellegrino C. Behavior of RC beams strengthened in shear with FRP and FRCM Composites. Eng Struct 2017; 150:830–42.
[119] National Cooperative Highway Research Program (NCHRP) Report 655. Recommended guide specification for the design of externally bonded FRP systems for repair and strengthening of concrete bridge elements. NCHRP Rpt 655. 2010. USA.
[120] ISIS. Design Manual No. 4 â€“ FRP rehabilitation of reinforced concrete structures. The Canadian network of centres of excellence on intelligent sensing for innovative structures (ISIS Canada). 2008.
[121] European Committee for Standardization. EN 1998-3 â€“ Eurocode 8 â€“ Design of structures for earthquake resistance â€“ Part 3: assessment and retrofitting of buildings. 2005.
[122] The Concrete Society (CS). TR55 Design guidance for strengthening concrete structures using fibre composite materials. January 2012. UK.
[123] Italian National Research Council (CNR). Guide for the design and construction of externally bonded FRP systems for strengthening existing structures: materials, RC and PC structures, masonry structures. CNR-DT 200 R1/2013. 2013. Rome, Italy.
[124] Japan Society of Civil Engineers (JSCE). Recommendations for upgrading of concrete structures with use of continuous fiber sheet. Concrete Engineering Series 2001;41. Japan.
[125] China association for Engineering Construction Standards (CECS). Technical specifications for strengthening structures with carbon fiber reinforced polymer laminates. Beijing, China: China planning press; 2003. CECS 146-2003.
[126] Egyptian Code of Practice (ECP). The use of fiber reinforced polymer (FRP) in the construction fields. ECP 208-2005. 2005. Egypt.
[127] ASTM. Standard methods of fire test of building construction and materials. West Conshohocken, PA: American Society for Testing and Materials; 2001. ASTM E119-01.